Handbook on the Physics and Chemistry of Rare Earths, edited by K.A. Gschneidner, Jr. and L. Eyring
© North-Holland Publishing Company, 1979

Chapter 24

THE ABSORPTION AND FLUORESCENCE SPECTRA OF RARE EARTH IONS IN SOLUTION

William T. CARNALL
Chemistry Division, Argonne National Laboratory, Argonne. IL 60439, USA

Contents

Symbols

ϵ = Molar absorptivity of an absorption band
F^k = Slater integral
ζ = Spin–orbit coupling integral
P = Oscillator strength
I, I_0 = Light intensity
σ = Energy of a transition (cm^{-1})
A = Transition probability (sec^{-1})
$\bar{F}^2$ = Electric dipole operator
$\bar{M}^2$ = Magnetic dipole operator
χ, χ' $\chi = (n^2+2)^2/9n$, $\chi' = n(n^2+2)^2/9$, where n is the bulk refractive index of the medium
T_λ = Intensity parameter defined in Judd–Ofelt theory

ν = Frequency of a transition (sec^{-1})
ψJ = Designation of a particular intermediately coupled SLJ electronic state in the f^N configuration
$U^{(\lambda)}$ = Unit tensor operator of rank λ
$\mathcal{T}_\lambda, \Omega_\lambda$ = Alternative forms of the intensity parameter T_λ defined by the Judd–Ofelt theory
α = All quantum numbers and suffixes in addition to SLJ needed to specify a particular state
δ = Kronecker delta
$\hbar$ = Planck's constant divided by 2π
β_R = Branching ratio for radiative relaxation to a particular final state
τ_R = Radiative lifetime of an excited state
τ_T = Total lifetime (radiative and non-radiative) of an excited state
W_T = Non-radiative relaxation rate of an excited state
ρ_E = Density of states

1. Introduction

1.1. *Scope*

This chapter deals almost exclusively with absorption and fluorescence spectra in aqueous solution. In outlining the present status of the experimental results and their theoretical interpretation, the attempt is made to identify those areas that are currently undergoing active development. Practically all of the experimental and interpretive techniques cited are directly applicable to investigations in non-aqueous solvents, but no effort has been made to cover that extensive literature.

Some of the main currents of thought that have contributed significantly to our present understanding of rare earth spectra in solution are outlined in the next section. At an early stage it was recognized that the spectra of certain members of the group serve as a sensitive probe to monitor changes in the ionic environment. Such spectra can provide one basis for the development of models of the structure of solutions.

The theoretical interpretation of solution spectra has undergone significant advances in recent years. It is now possible to compute both the energies and intensities of bands in good agreement with experiment. While the intensity calculations normally involve parameters evaluated from experimental data, these parameters can be calculated from first principles based on a model for at least the immediate environment of the ion. Some attempts have been made to explore the type of model required by the intensity theory, but the problem is complex and progress along these lines has been slow. At present it appears that intensity correlations play a much more immediate role in the interpretation of the mechanisms of relaxation of excited states of the ions in solution. The concepts involved have been widely applied in investigations of lanthanide lasers.

1.2. *Historical development*

Although many published accounts of research involving the spectra of lanthanide ions in solution predate the 1930's, this was the era of extensive development that provided the basis for many concepts that are still under active investigation. In one of the classic papers in rare earth spectroscopy, the outgrowth of many years' effort to purify materials, Prandtl and Scheiner (1934) presented an essentially complete collection of trivalent lanthanide solution absorption spectra. This collection, covering the region 7000–2000 Å, stimulated and influenced the thinking of many subsequent investigators at a time when the theoretical interpretation of such spectra was just developing. The authors emphasized an apparent symmetry in region of absorption with band structure shifting toward the ultraviolet in approaching the center of the series from both ends.

Ce (colorless)
Pr (yellow green)
Nd (red violet)
61 (unknown)
Sm (yellow)
Eu (essentially colorless)
Gd (colorless)
Tb (essentially colorless)
Dy (light yellow green)
Ho (brownish yellow)
Er (pink)
Tm (light green)
Yb (colorless)

This apparent symmetry, which had been pointed out earlier by Main-Smith (1927) based on color alone, led to the expectation that bands for members at the beginning and end of the series might be found in the infrared region. Indeed several such observations were noted.

Three years later, interpretation of lanthanide spectra was placed on a much firmer basis when Van Vleck (1937) summarized the evidence for attributing the sharp absorption bands observed in both solutions and solids to transitions within the $4f^N$ configuration. While a number of investigators had espoused this interpretation (Freed, 1931; Tomaschek, 1932; Lang, 1936; Mukherji, 1936), it was by no means universally accepted. Van Vleck pointed out that the intensities reported for Pr^{3+} and Nd^{3+} absorption bands were a factor of 10^6 weaker than would have been expected for normal electric dipole transitions, and concluded that there were probably several contributing mechanisms that could account for the magnitude of the observed transitions.

Progress was also being made during this period in the theoretical interpretation of the spectra of rare earth compounds and solutions in terms of energy level structure as Bethe and Spedding (1937), Lange (1938), and Spedding

(1940) published analyses of the free-ion energy level schemes in $Pr^{3+}(4f^2)$ and $Tm^{3+}(4f^{12})$. Differences in interpretation were not fully resolved in favor of the intra f-configuration concept until later, when Broer et al. (1945) reexamined Van Vleck's arguments and revised some of the intensity estimates. It was not until 1953 that the energy level analysis was extended to more complex spectra when Satten (1953) undertook the analysis of $Nd^{3+}(4f^3)$. Jørgensen (1955) was one of the first to attempt to identify systematically lanthanide aquo ion energy levels.

While to a first approximation, the spectra of the lanthanides in solution were known to be rather insensitive to the environment, the significance of the relatively small but distinctive changes that could be induced in certain absorption bands was pointed out at an early stage. The smaller number of lines observed in bands in $Eu(NO_3)_3$ solution compared to those in $EuCl_3$ solution led Freed and Weissman (1938) to ascribe a higher symmetry to the immediate environment in the nitrate case. Freed (1942) summarized much of the early work on environmental effects in both crystals and solutions.

In a series of papers published from the Zeeman Laboratory in Amsterdam in the early 1940's, quantitative measurements of the solution absorption spectra of the lanthanides, corrected for known impurities in the samples, were made. This constituted the first systematic investigation of band intensities (oscillator strengths) for these ions (Woudenberg, 1942a,b; Franzen et al., 1943; Hoogschagen et al., 1943, 1946a,b; Hoogschagen, 1946; Hoogschagen and Gorter, 1948). Based on the relative magnitudes of the electrostatic and spin-orbit interactions, Bethe and Spedding (1937), and Spedding (1940), Broer et al. (1945) concluded that the energy levels must be treated in the intermediate coupling approximation, i.e., J is a good quantum number, but L and S are not. It was also noted that the J and g-values associated with the ground states deduced from magnetic data agreed with those calculated from Hund's rule.

While much of the data published prior to 1945 is accurate and consistent with more recent results, there have been significant improvements in both purity of materials and in the resolution of recording spectrophotometers. Comprehensive investigations of lanthanide spectra have been published by Moeller and Brantley (1950), Holleck and Hartinger (1955), Banks and Klingman (1956) and Stewart (1959), and extended to the near infrared region by Carnall et al. (1962, 1964) and Carnall (1963).

Along with the increased availability of quantitative measurements of band intensities and energies in solution, there has been a rapid development in the theoretical interpretation of the energy level structures of the lanthanide ions. Much of the latter is based primarily on experimental results obtained with single crystals (Dieke (1968)).

Exciting new possibilities for interpretation of the fundamental processes of absorption and emission of radiation by lanthanide ions in solution were opened up by the publication by B.R. Judd (1962) and independently by G.S. Ofelt (1962) of a theory which made possible quantitative interpretation of intensities associated with observed absorption bands. This development has played a decisive role in much of the subsequent research involving the spectra of these ions.

2. Absorption spectra in solution

2.1. *Nature of the transitions*

Systematic variation in the energy differences between the lowest levels of the $4f^N$ and higher-lying configurations in various ionization states of the lanthanides was pointed out almost simultaneously by Brewer (1971a,b), Nugent and Vander Sluis (1971), and Martin (1971). For the trivalent lanthanides, the emission spectroscopic results establish $4f^N$ as the ground configuration. The lowest energy level belonging to the next higher ($4f^{N-1}5d$) configuration follows the trend shown in fig. 24.1. In solution, the energy of these $4f \rightarrow 5d$ transitions is lowered by $\sim 15000\,cm^{-1}$ compared to that of the gaseous ion, and the corresponding relatively intense (parity allowed) bands can be observed in the ultraviolet region for Ce^{3+}(aquo), Pr^{3+}(aquo), and Tb^{3+}(aquo). As indicated in fig. 24.1, the electronic absorption spectra for most of the 3+ lanthanides within the spectral range normally observed (to 200 nm), only involves transitions within the $4f^N$-configuration.

In several rare earth ions, Sc^{3+}, Y^{3+}, La^{3+}, Ce^{4+}(iso-electronic with La^{3+}), and Lu^{3+}, the core electronic structure comprises completely filled shells. In such cases, no electronic absorption spectra at >200 nm is expected because the corresponding process of promoting an electron out of a filled shell requires much higher energies. Broad absorption that appears to increase exponentially is observed in the ultraviolet region of a number of rare earth ions and is particularly apparent in Eu^{3+}(aquo), Yb^{3+}(aquo) and Ce^{4+}(aquo). For complexes

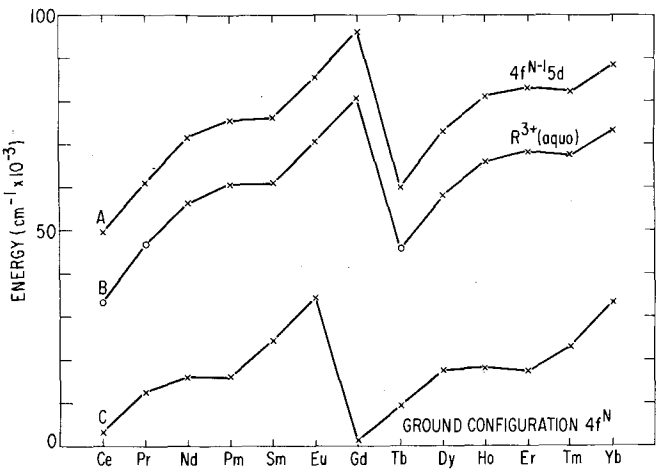

Fig. 24.1. Energy of the lowest level in the $4f^{N-1}5d$ configuration relative to that of $4f^N$ for the lanthanides. (A) Lanthanide 3+ gaseous ion spectra (Brewer, 1971). (B) Data of (A) corrected to spectra observed in dilute acid solution. The results for Ce^{3+}(aquo), Pr^{3+}(aquo) and Tb^{3+}(aquo) are experimental (Jørgensen and Brinen, 1963). (C) Lanthanide 2+ gaseous ion spectra. For Gd^{2+}, the $4f^7$5d-configuration lies lowest and the $4f^8$ is at $1500\,cm^{-1}$ (Brewer, 1971).

such as $CeCl_6^{-2}$ and $CeBr_6^{-2}$, pronounced absorption bands are apparent, and they extend well into the visible range (Ryan and Jørgensen, 1966). The absorption mechanism involved in these cases is the electron transfer process (Jørgensen and Brinen, 1963; Jørgensen, 1973), where in general the absorption of energy results in the transfer of an electron from molecular orbitals on the ligands to the nl-shell of the central atom.

Those divalent lanthanides whose absorption spectra have been observed under normal conditions in solution, $Sm^{2+}(4f^6)$, $Eu^{2+}(4f^7)$, and $Yb^{2+}(4f^{14})$ (Butement, 1948), have much lower-lying $4f^{N-1}5d$ configurations than is the case with the trivalent ions which possess the corresponding f^N configuration (Brewer, 1971b), fig. 24.1. In all three cases, only the $f \rightarrow d$ transitions are actually observed in solution. The weak $f \rightarrow f$ transitions in Sm^{2+} and Eu^{2+} that are expected to occur in the visible-ultraviolet region are lost in the strong $f \rightarrow d$ bands.

2.2. *Absorption spectra of* R^{3+} *ions. Experimental results*

The region of the spectrum in which lanthanide absorption bands can be observed in aqueous solution is restricted as indicated in fig. 24.2. In the ultraviolet range, aqueous solvents are suitable to ~200 nm, which is also the usual spectrophotometer limit. Absorption bands characteristic of Pr^{3+}, Nd^{3+}, Sm^{3+}, Dy^{3+}, Ho^{3+}, and Er^{3+} in the 900–1100 nm range in aqueous solution were

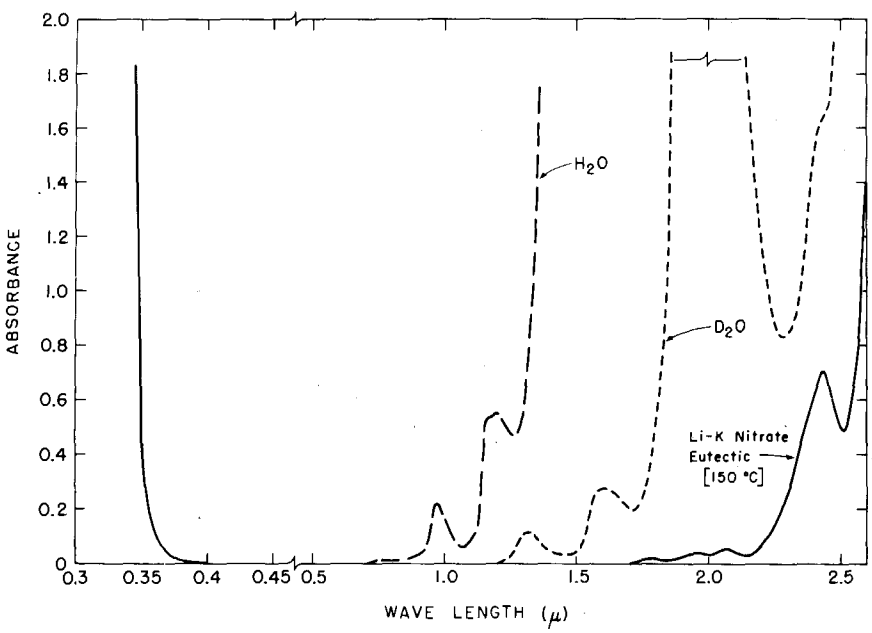

Fig. 24.2. Comparative absorption spectra of different solvent systems in 1 cm path length cells.

reported at a very early date (Freymann and Takvorian, 1932). Stewart (1959) extended observations to the ~1400 nm cut-off in H_2O in his systematic investigation. More extensive spectra using D_2O as the solvent, published by Carnall et al. (1962, 1964), Carnall (1963), revealed a number of bands in the ~1400–1800 nm region. The same authors further extended observations to ~2600 nm by using the molten $LiNO_3$-KNO_3 eutectic (~150°C) as a solvent, and the advantages of using characteristic bands in this region in the analysis of mixtures of lanthanides were pointed out (Carnall, 1962).

Fused salts have been a popular solvent medium for lanthanide ion spectroscopy. Typical systematic investigations were carried out in molten fluorides (Young and White, 1960a,b) and in molten chlorides (Banks et al., 1961). Measurements in the LiCl-NaCl-KCl eutectic (333°C) included the near infrared range (Mamiya, 1965), and a more comprehensive investigation was carried out in LiCl-KCl eutectic at 450°C (Johnson and Sandoe, 1968). The oxidizing character of the nitrate melt makes it an ideal medium for stabilizing the trivalent state of the lanthanides at 150–200°C, whereas in the chloride melt, some evidence of reduction or charge transfer absorption is noted in the spectra of the most easily reduced species, Sm^{3+}, Eu^{3+}, and Yb^{3+}. Lanthanide absorption spectra covering a range similar to that observed in the $LiNO_3$-KNO_3 eutectic at 150°C have also been recorded in non-aqueous solvents at 25°C (Heller, 1968).

The absorption spectra shown in figs. 24.3–24.15 represent a consistent set of results in dilute $HClO_4$ or $DClO_4$ solution. In cases where the f→f transitions are superimposed on broad bands that are attributed to other processes such as charge transfer or f→d transitions, the background absorption has been subtracted where possible.

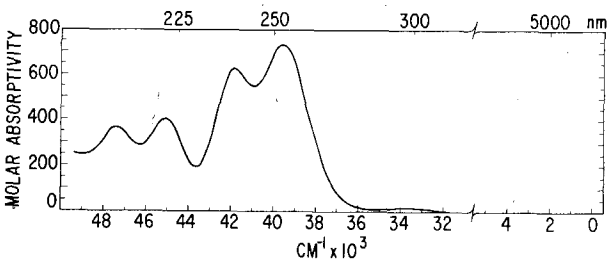

Fig. 24.3. Solution absorption spectrum of Ce^{3+}(aquo). Jørgensen and Brinen (1963) report an additional band at 200 nm (50000 cm^{-1}) not shown.

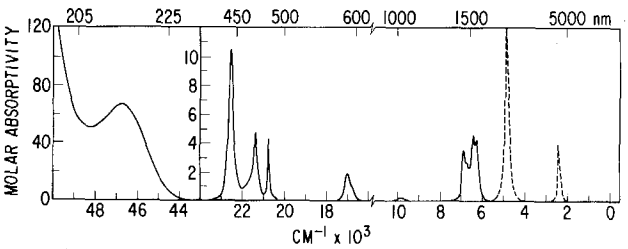

Fig. 24.4. Solution absorption spectrum of Pr^{3+}(aquo). Dashed lines indicate calculated curves (section 3.7).

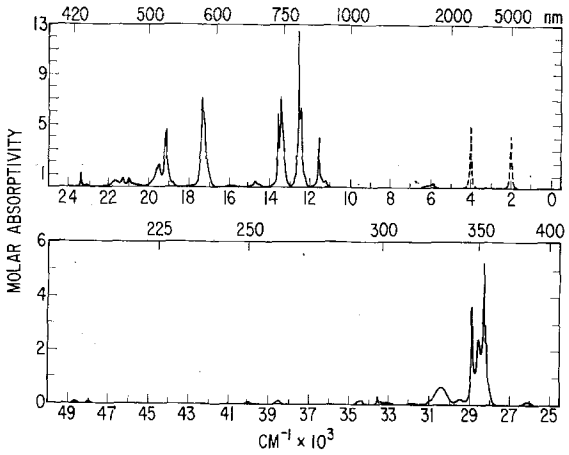

Fig. 24.5. Solution absorption spectrum of Nd^{3+}(aquo). Dashed lines indicate calculated curves (section 3.7).

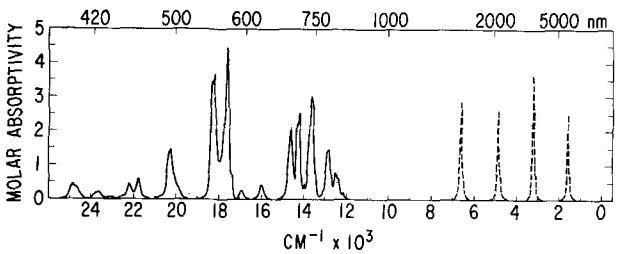

Fig. 24.6. Solution absorption spectrum of Pm^{3+}(aquo). Dashed lines indicate calculated curves (section 3.7).

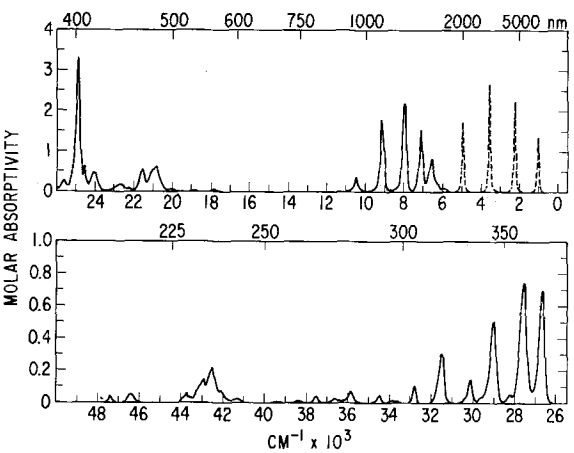

Fig. 24.7. Solution absorption spectrum of Sm^{3+}(aquo). Dashed lines indicate calculated curves (section 3.7).

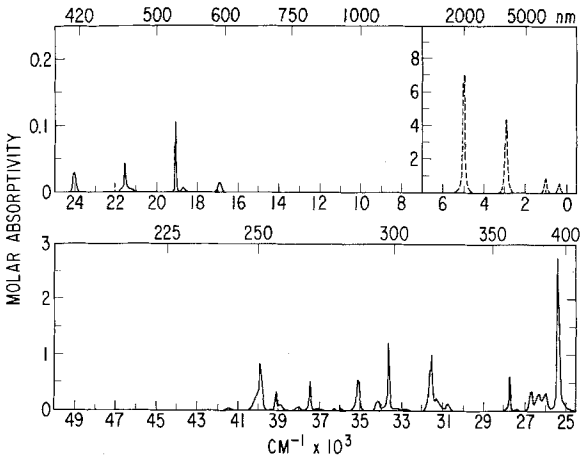

Fig. 24.8. Solution absorption spectrum of Eu^{3+}(aquo). Dashed lines indicate calculated curves (section 3.7).

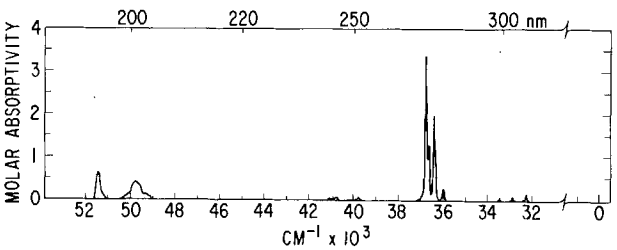

Fig. 24.9. Solution absorption spectrum of Gd^{3+}(aquo).

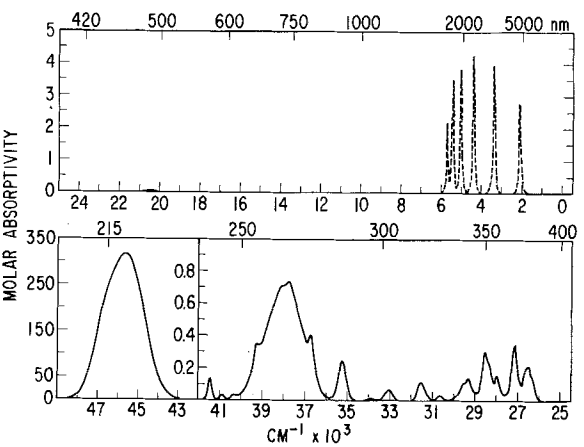

Fig. 24.10. Solution absorption spectrum of Tb^{3+}(aquo). Dashed lines indicate calculated curves (section 3.7).

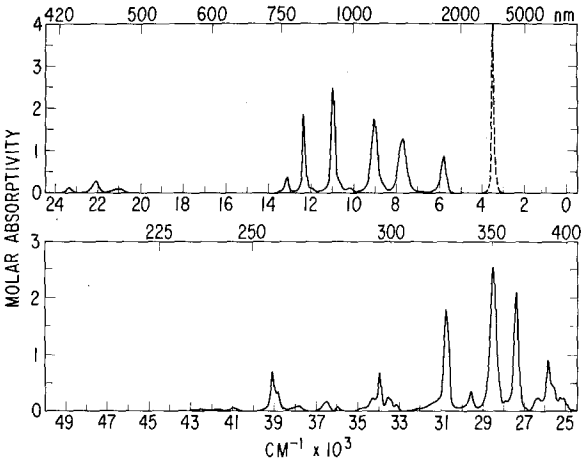

Fig. 24.11. Solution absorption spectrum of Dy^{3+}(aquo). Dashed lines indicate calculated curves (section 3.7).

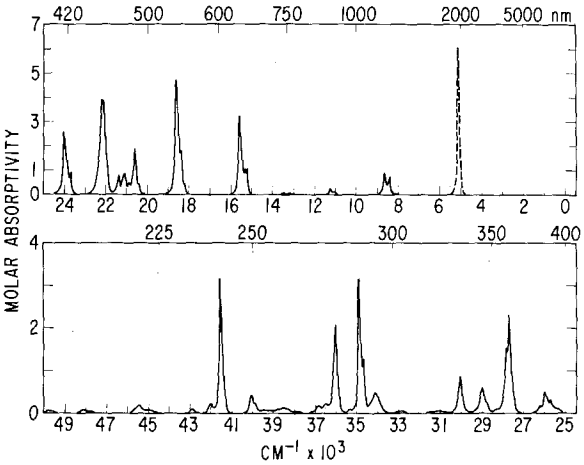

Fig. 24.12. Solution absorption spectrum of Ho^{3+}(aquo). Dashed lines indicate calculated curves (section 3.7).

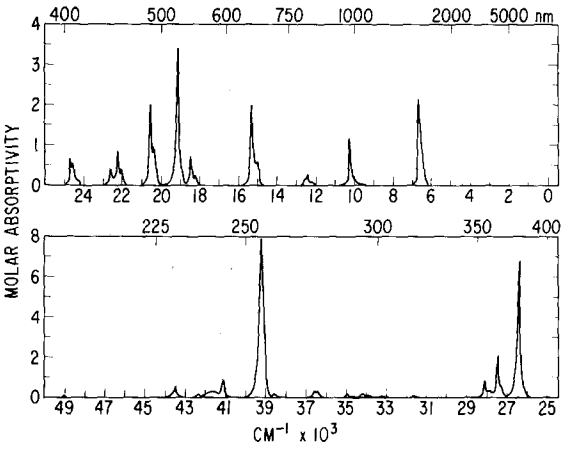

Fig. 24.13. Solution absorption spectrum of Er^{3+}(aquo).

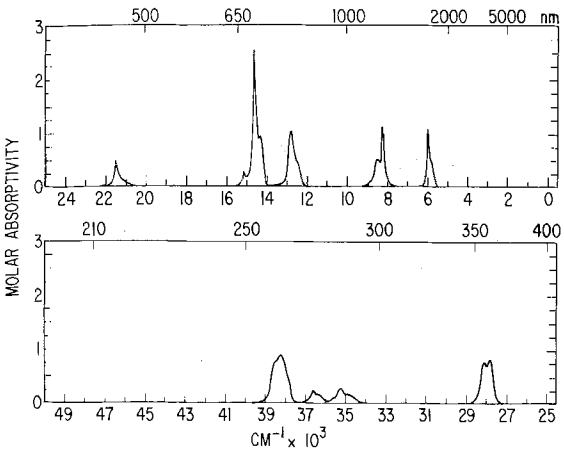

Fig. 24.14. Solution absorption spectrum of Tm^{3+}(aquo).

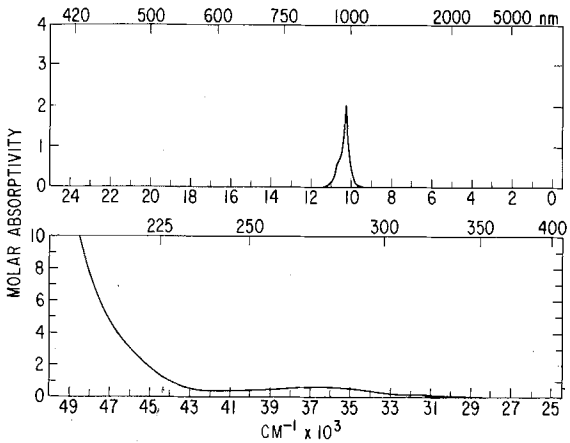

Fig. 24.15. Solution absorption spectrum of Yb^{3+}(aquo).

As noted earlier, bands characteristic of the lanthanides are observed in non-aqueous solvents at lower energies than is possible in $DClO_4$. In a subsequent section, the quantitative treatment of band intensities is discussed. As a result of this work, the energies and intensities of all the transitions characteristic of the lanthanides in aqueous solution in the energy range 0–5500 cm^{-1} can be computed. The corresponding bands are included in the spectra shown in figs. 24.4–24.12 and discussed in section 3.7.

A band register which includes the molar absorptivities (ϵ) for all trivalent lanthanide absorption band maxima with $\epsilon > 0.2$ is given in table 24.1. The region of the spectrum covered is that which can be observed in H_2O and D_2O.

TABLE 24.1
Band register for R^{3+}(aquo) ions in H_2O–D_2O with molar absorptivity (ϵ) > 0.2.

Band peak				Band peak			
(cm^{-1})	(nm)[a]	Ion	ϵ	(cm^{-1})	(nm)[a]	Ion	ϵ
5837	1713	Dy	0.84	15608	641	Ho	3.19
5988	1670	Nd	0.25	16000	625	Pm	0.44
6006	1665	Tm	1.04	16920	591	Pm	0.26
6309	1585	Pr	4.18	16980	589	Pr	1.88
6451	1550	Pr	4.51	17373	576	Nd	7.20
6622	1510	Sm	0.79	17605	568	Pm	4.43
6667	1500	Er	2.11	18215	549	Er	0.21
6896	1450	Pr	3.60	18235	548	Pm	3.68
7143	1400	Sm	1.54	18315	546	Pm	3.45
7707	1297	Dy	1.22	18399	544	Ho	1.81
8051	1242	Sm	2.02	18477	541	Er	0.72
8278	1208	Tm	1.11	18632	537	Ho	4.74
8417	1188	Ho	0.74	19128	523	Er	3.40
8529	1172	Tm	0.50	19198	521	Nd	4.33
8673	1153	Ho	0.87	19522	512	Nd	1.76
9066	1103	Dy	1.72	20242	494	Pm	1.47
9199	1087	Sm	1.77	20375	491	Er	0.93
9876	1012	Pr	0.20	20542	487	Er	2.02
10262	974	Yb	2.03	20614	485	Ho	1.84
10262	974	Er	1.14	20772	481	Pr	4.29
10520	951	Sm	0.36	20833	480	Ho	0.48
10995	910	Dy	2.44	20894	479	Sm	0.60
11235	890	Ho	0.22	21017	476	Nd	0.72
11556	865	Nd	4.01	21106	474	Ho	0.82
12398	806	Dy	1.82	21308	469	Nd	0.78
12462	802	Er	0.27	21349	468	Pr	4.59
12472	802	Nd	6.42	21377	468	Ho	0.82
12484	801	Pm	0.74	21533	464	Tm	0.48
12586	794	Nd	12.5	21580	463	Sm	0.54
12804	781	Pm	1.46	21668	462	Nd	0.52
12820	780	Tm	1.02	21786	459	Pm	0.63
13210	757	Dy	0.35	22056	453	Er	0.38
13508	740	Nd	7.27	22065	453	Dy	0.26
13624	734	Pm	3.04	22185	451	Ho	3.90
13665	732	Nd	5.93	22222	450	Pm	0.46
13980	715	Pm	0.48	22242	450	Er	0.88
14239	702	Pm	2.54	22522	444	Pr	10.4
14347	697	Tm	0.92	22624	442	Er	0.43
14600	685	Nd	0.22	23386	428	Nd	1.14
14625	684	Pm	2.11	23640	423	Pm	0.20
14663	682	Tm	2.43	23708	422	Ho	0.89
14721	679	Nd	0.50	24033	416	Ho	2.55
15015	666	Er	0.54	24096	415	Sm	0.47
15179	659	Tm	0.27	24570	407	Er	0.53
15238	656	Ho	1.03	24582	407	Sm	0.61
15314	653	Ho	1.01	24704	405	Er	0.67
15328	652	Er	1.97	24876	402	Pm	0.46

TABLE 24.1. (*Contd.*)

Band peak				Band peak			
(cm^{-1})	(nm)[a]	Ion	ϵ	(cm^{-1})	(nm)[a]	Ion	ϵ
24925	401	Sm	3.31	31505	317	Eu	1.01
25227	396	Dy	0.23	31546	317	Sm	0.31
25419	393	Eu	2.77	33580	298	Dy	0.21
25602	390	Sm	0.26	33580	298	Nd	0.33
25680	389	Ho	0.29	33602	298	Eu	1.21
25840	387	Dy	0.89	33944	295	Dy	0.67
25974	385	Ho	0.49	34153	293	Ho	0.47
25988	385	Eu	0.33	34320	291	Dy	0.22
26330	380	Eu	0.31	34420	290	Nd	0.27
26334	379	Dy	0.24	34674	288	Ho	1.26
26385	379	Er	6.68	34891	287	Ho	3.16
26510	377	Tb	0.21	35100	285	Eu	0.57
26624	376	Eu	0.36	35211	284	Tm	0.27
26702	374	Eu	0.36	35223	284	Tb	0.25
26752	374	Sm	0.70	35920	278	Gd	0.29
27137	368	Tb	0.34	35997	278	Ho	2.07
27427	365	Dy	2.11	36258	276	Gd	0.92
27457	364	Er	2.08	36337	275	Gd	2.00
27624	362	Sm	0.75	36443	274	Er	0.31
27678	361	Eu	0.64	36536	274	Gd	1.38
27716	361	Ho	2.27	36550	274	Ho	0.20
27809	360	Tm	0.80	36576	273	Gd	1.22
27932	358	Er	0.31	36576	273	Tm	0.23
28090	356	Tm	0.76	36603	272	Er	0.30
28120	356	Er	0.85	36710	272	Gd	3.41
28296	353	Nd	5.30	37439	267	Eu	0.54
28545	350	Tb	0.31	38226	262	Tm	0.90
28555	350	Nd	2.46	38490	260	Nd	0.22
28556	350	Dy	2.54	38850	257	Dy	0.32
28892	346	Nd	3.71	39093	256	Dy	0.68
28985	345	Ho	0.59	39108	256	Eu	0.35
29070	344	Sm	0.50	39200	255	Er	7.89
29410	340	Nd	0.21	39872	251	Eu	0.80
29595	338	Dy	0.34	40064	250	Ho	0.39
30039[b]	333	Pm	4.73	41152	243	Er	0.89
30048	333	Ho	0.82	41560	241	Ho	3.16
30469	328	Nd	0.68	41666	240	Er	0.31
30478[b]	328	Pm	4.96	42016	238	Ho	0.21
30798	325	Dy	1.78	42553	235	Sm	0.22
31250[b]	320	Pm	2.53	43525	230	Er	0.58
31270	320	Eu	0.24				

[a]Measured center of observed band. The value in cm^{-1} is the converted value; [b]Gruber and Conway (1960).

2.3. *Absorption spectra of* R^{2+} *ions. Experimental results*

Since the lanthanides that exhibit the divalent state in aqueous solution, Sm^{2+}, Eu^{2+}, and Yb^{2+}, are all readily oxidized to the trivalent state, attempts to record their absorption spectra have usually proceeded from the rapid dissolution of a soluble anhydrous compound. The absorption spectra shown in fig. 24.16 for Sm^{2+}, Eu^{2+}, and Yb^{2+} were adapted from results published by Butement and Terrey (1937), Butement (1948), and Christensen et al. (1973). Production of other divalent lanthanide ions by pulse radiolysis, and the observation of their spectra is discussed in section 5.2.

3. Theoretical treatment of 3+ lanthanide solution absorption spectra

We are concerned here exclusively with the trivalent lanthanides since there has been little progress made beyond a general interpretation of the band structure observed in solutions containing the divalent ions. Two aspects of the interpretation of the spectra will be considered. First, the energy level structure is calculated in agreement with experiment using a model that includes sufficiently high order interactions to insure accurate intermediate coupling eigenvectors for states over the whole energy range of observation. Second, the intensities of the observed bands are related to a semi-empirical theory, which in turn can be used to predict properties of the absorption and fluorescence spectra. The parameters of the intensity theory can be calculated on a first

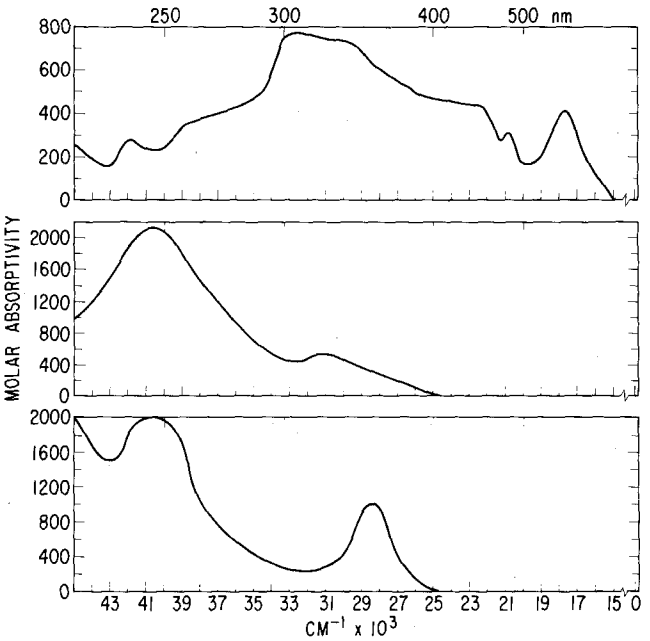

Fig. 24.16. Solution absorption spectra of Sm^{2+}(aquo), Eu^{2+}(aquo), and Yb^{2+}(aquo) adapted from Butement (1948).

principles basis, but in practice this approach suffers from the same lack of an accurate model of the environment that limits the first principles computation of lanthanide crystal-field parameters.

3.1. *Energy level calculations*

A number of sources present extensive development of the energy level structure theory in lanthanide spectra, but works by Wybourne (1965), Judd (1963), and Dieke (1968) are particularly useful. Only a brief summary that includes recent developments in the theoretical model will be included here.

Since for present purposes interest is entirely centered on transitions within the $4f^N$ configuration, it can be taken as a good simplifying approximation that electrons in closed shells in a lanthanide ion exert a constant influence on all of the f^N-states. The problem then is to identify those effective interactions operating within the f^N configuration that reproduce the observed structure. The principal terms of the current model can be written:

$$E = \sum_{k=0}^{6} F^k(nf, nf) f_k + \zeta_{4f} A_{SO} + E_{CI} + E_{CF} \qquad (k \text{ even}) \tag{24.1}$$

where f_k and A_{SO} represent the angular parts of the electrostatic and spin–orbit interactions, respectively. The F^k are Slater integrals, $F^2 = 225F_2$, $F^4 = 1089F_4$, and $F^6 = 184\,041/25F_6$, representing the purely electrostatic interaction between the f electrons, and ζ_{4f} is the spin-orbit coupling constant. The term E_{CI} is used here to represent the two-body and three-body effective operators that have been added to the model in recent years to account for the effects of configuration mixing, and E_{CF} is the crystal or ligand field interaction term.

The relative magnitudes of the principal terms in eq. (24.1) are indicated in fig. 24.17 which shows the experimentally well established energy level scheme for $Pr^{3+}:LaCl_3$ (Dieke, 1968). The fact that several of the excited states in $Pr^{3+}:LaCl_3$ are isolated in energy, makes it possible to identify the transitions responsible for the corresponding absorption bands in fig. 24.4.

While the principal interactions that give rise to the structure of the f^N configuration are the electrostatic and spin–orbit terms of eq. (24.1), and the corresponding degenerate states are the free-ion states, computation of the energies of spectroscopic states based solely on these interactions are only approximate. Even in the relatively simple case of $Pr^{3+}(4f^2)$, differences between observed and calculated free-ion levels of $>500\ cm^{-1}$ are encountered (Spedding, 1940; Carnall, 1974).

In recent analyses of lanthanide spectra, the term E_{CI} in eq. (24.1) has included the effects of configuration interaction as expressed in the Trees correction $\alpha L(L+1)$, and the parametrized Casimir operators $\beta G(G_2)$ and $\gamma G(G_7)$ (Trees, 1964; Rajnak and Wybourne, 1963). The additional terms represent those effects of configuration interaction that can be accounted for by two-body effective operators that do not transform as the f_k in eq. (24.1). For configurations of three or more equivalent f-electrons, the three-particle operators of Judd (1966a), $T^i t_i$

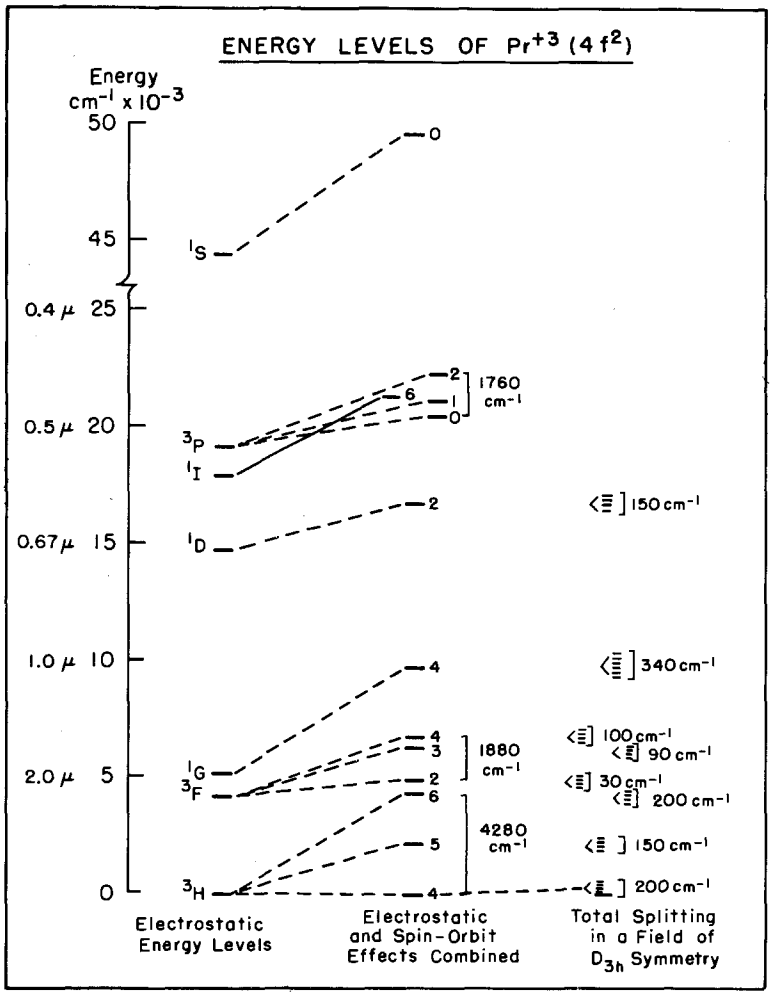

Fig. 24.17. Schematic energy level structure for $Pr^{3+}(4f^2)$.

($i = 2,3,4,6,7,8$) where T^i are the parameters and t_i are the operators, have been included to account for the perturbing influence of those configurations that differ from f^N in the quantum numbers of a single electron. In addition to the electrostatically correlated interactions, Judd et al. (1968) have provided the basis for including a number of magnetically correlated interactions in the parametric analysis. The effects represented by E_{CI} are not small. They may shift the energies of individual terms by several hundred wavenumbers.

Approximate values for the radial integrals associated with the electrostatic and spin–orbit interactions can be obtained from both relativistic and non-

relativistic Hartree–Fock methods (Lewis et al., 1970; Crosswhite and Cowan, 1976). Such computed values are in general too large because they do not include the effects of configuration interaction. They may be scaled down by systematic comparison with results obtained semi-empirically. The magnitudes of some of the important parameters of configuration interaction and the screening of the electrostatic integrals have also been computed (Morrison and Rajnak, 1971; Newman and Taylor, 1971, 1972). However, all of these integrals are in practice treated as parameters to be evaluated from experimental data. The angular parts of the interactions can be calculated exactly using Racah's tensor operator methods (Judd, 1963). The *ab initio* methods do, however, yield values for the parameters of configuration interaction that are in good agreement with those obtained by parameterization, and thus tend to confirm the validity of the latter procedure.

Recent investigations of the spectra of $Nd^{3+}:LaCl_3$ (Crosswhite et al., 1976), and $Pm^{3+}:LaCl_3$ (Carnall et al., 1976), provide examples of the results obtained using the expanded parameterization model. The fits to observed "free-ion" states have an RMS deviation of $<20\,cm^{-1}$, and the parameter values exhibit regular trends over the whole lanthanide series (Crosswhite et al., 1975).

The fact that 4f-electrons are well shielded from the environment by filled $5s^2$ and $5p^6$ shells (Wybourne, 1965), results in there being a close similarity in the level structure derived from the analysis of lanthanide spectra in crystalline solids such as $R^{3+}:LaCl_3$ and that observed for the R^{3+}(aquo) ion. Indeed evidence was presented at an early stage to show that the spectroscopic properties of Eu^{3+} ions in solution at reduced temperature were very similar to those of the ions in crystals (Freed and Weissman, 1938). Subsequent experiments with mixed component solutions containing Eu^{3+} (Sayre et al., 1957), and Nd^{3+} and Sm^{3+} (Freed and Hochanadel, 1950), demonstrated the continuity between the numerous sharp lines which could be identified as crystal-field components in a microfield of clearly defined site symmetry in solution at low temperature, and the band envelope of these lines that developed as the temperature was raised.

For solution spectra at room temperature, the term in eq. (24.1) which expresses the effects of the crystal field is not included. Instead what is calculated is the center of gravity of the absorption bands. While the term "free-ion" calculation is used, the level scheme is clearly not that that would be characteristic of the gaseous free-ion. Each different medium shifts the center of gravity of the envelopes of crystal-field components to slightly different energies. This screening effect on the f-electrons has been referred to by Jørgensen (1969) as the nephelauxetic effect.

Values of the energy level parameters obtained from a fit to lanthanide solution absorption spectra are given in table 24.2 (Carnall et al., 1968a). While more accurate values can now be derived from a consistent treatment of data in crystals, the indicated results constitute a useful set for computing eigenvectors of states in intermediate coupling as required in the intensity calculations to be discussed next.

TABLE 24.2.
Energy level parameter values calculated for the R^{3+}(aquo) ions[a] (in cm^{-1})

	F^2	F^4	F^6	ζ_{4f}	α	β	γ
Pr^{3+}	68674	50395	32648	740.75	21.255	−799.93	1342.9
Nd^{3+}	72412	50394	34698	884.58	0.5611	−117.15	1321.3
Pm^{3+} [b]	76585	54538	35135	1022.8	20.692	−616.29	1967.5
Sm^{3+}	82008	61766	39922	1157.3	22.250	−742.55	796.64
Eu^{3+}	83162	61245	41526	1326.0	25.336	−580.25	1155.7
Gd^{3+}	86625	62890	42513	1450.0	22.552	−103.7	996.98
Tb^{3+}	90358	66213	44262	1709.5	20.131	−370.21	1255.9
Dy^{3+}	91730	65886	46194	1932.0	37.062	−1139.1	2395.3
Ho^{3+}	94448	70849	49835	2141.3	23.635	−807.20	1278.4
Er^{3+}	99182	72778	53812	2380.7	18.347	−509.28	649.71
Tm^{3+}	103887	77024	57449	2628.7	14.677	−631.79	—

[a]Carnall et al. (1968a). [b]Free-ion parameters from data for Pm^{3+}:$LaCl_3$ (Carnall et al., 1976).

3.2. *Experimental determination of intensities of absorption bands*

The quantitative treatment of the intensities of 3+ lanthanide absorption bands relates an experimentally determined quantity, a normalized band envelope, to a theoretical model based on the mechanisms by which radiation can be absorbed. The integrated absorption bands observed in a solution of known concentration can be used to calculate the number of classical oscillators in one ion, which is more commonly referred to as the probability for absorption of radiant energy P (oscillator strength) by the expression (Hoogschagen, 1946):

$$P = \frac{2303\, mc^2}{N\pi e^2}\int \epsilon_i(\sigma)\, d\sigma = 4.32 \times 10^{-9}\int \epsilon_i(\sigma)\, d\sigma \tag{24.2}$$

where ϵ_i is the molar absorptivity of a band at the energy $\sigma(cm^{-1})$, and the other symbols have their usual meaning. P is here a dimensionless quantity. The molar absorptivity at a given energy is computed from the Beer–Lambert law:

$$\epsilon = \frac{1}{cl}\log I_0/I \tag{24.3}$$

where c is the concentration of the lanthanide ion in moles/liter, l is the light path in the solution (cm), and $\log I_0/I$ is the absorptivity or optical density. Maximum molar absorptivities of lanthanide absorption bands in dilute non-complexing acid solution are usually <10 and average nearer unity as shown in table 24.1. Oscillator strengths are in general of the order of 1×10^{-6}.

3.3. *Model calculation of absorption intensity. General considerations*

As Van Vleck (1937) and Broer et al. (1945) pointed out, there is some magnetic dipole character in a few transitions (P_{MD}), but an induced electric–

dipole mechanism (P_{ED}) must be invoked to account for the intensities of most lanthanide absorption bands. The term induced or forced electric dipole is used to emphasize that true electric dipole transitions require the initial and final states to be of different parity, whereas no parity change is involved in transitions *within* a configuration. In contrast, magnetic dipole transitions within a configuration are (parity) allowed. The weak intra f^N transitions are thus accounted for by assuming that a small amount of the character of higher-lying opposite parity configurations is mixed into the f^N states via the odd terms in the potential due to the ligand field (Wybourne, 1965). We can therefore write $P_{expt} = P_{ED} + P_{MD}$.

In view of the interest in both absorption and fluorescence processes in solution, there is an advantage in pointing out the basic role of the Einstein coefficient in expressing the transition probability due to dipole radiation:

$$A(\mathrm{i}, \mathrm{f}) = \frac{64\pi^4\sigma^3}{3h} |\langle \mathrm{i}|\boldsymbol{D}|\mathrm{f}\rangle|^2 \tag{24.4}$$

where i and f signify the initial and final states, A is the (spontaneous) transition probability per unit time, σ (cm^{-1}) is the energy difference between the states, and $\boldsymbol{D}$ is the dipole operator (Condon and Shortley, 1957).

In addressing the problem of the absorption of energy, Broer et al. (1945) expressed eq. (24.4) in terms of oscillator strength using the relationship $P = Amc/8\pi^2\sigma^2e^2$. The factor $2J + 1$ was added since the matrix elements of $\boldsymbol{D}$ are summed over all components of the initial state i. A refractive index correction χ was also included giving:

$$P = \frac{8\pi^2 mc\sigma}{3he^2(2J+1)} [\chi \bar{F}^2 + n\bar{M}^2] \tag{24.5}$$

where $\bar{F}^2$ and $\bar{M}^2$ represent the matrix elements of the electric dipole and magnetic dipole operators, respectively, joining an initial state J to the final state J', $\chi = (n^2+2)^2/9n$, and n is the refractive index of the medium.

3.4. *Induced electric dipole transitions*

Judd (1962) and Ofelt (1962) independently derived expressions for the oscillator strength of induced electric dipole transitions within the f^N configuration. This was a signal accomplishment. Much of the highly significant theoretical interpretation of the fluorescence process and the prediction of the properties of solid state lanthanide lasers, ch. 35, was made possible by this work. Since their results are similar, and were published simultaneously, the basic theory has become known as the Judd–Ofelt theory. However, Judd's expression, eq. (24.6), was cast in a form that could be directly related to oscillator strengths derived from lanthanide solution spectra, and he was the first to show that the model satisfactorily reproduced the experimental results for Nd^{3+}(aquo) and

Er^{3+}(aquo).

$$P_{ED} = \sum_{\lambda=2,4,6} T_\lambda \nu (\psi J \| U^{(\lambda)} \| \psi' J')^2 \tag{24.6}$$

where $\nu(\sec^{-1})$ is the frequency of the transition $\psi J \rightarrow \psi' J'$, $U^{(\lambda)}$ is a unit tensor operator of rank λ, the sum running over the three values $\lambda = 2,4,6$, and the T_λ are three parameters which can be evaluated from experimental data. These parameters involve the radial parts of the $4f^N$ wave functions, the wave functions of perturbing configurations such as $4f^{N-1}5d$, and the interaction between the central ion and the immediate environment.

In order to facilitate the intercomparison of parameters for different lanthanide ions, eq. (24.6) was modified by the substitution $T_\lambda = \mathcal{T}_\lambda/2J + 1$, and results for all of the lanthanides in dilute acid solution have been reported in terms of $\mathcal{T}_\lambda$ (Carnall et al., 1965, 1968b). However, those investigators who have studied lanthanide intensities in crystals have followed an alternate parameterization proposed by Axe (1963). The latter has clear advantages in describing both the absorption and fluorescence processes in terms of a single set of adjustable parameters.

The expression for T_λ given by Judd was:

$$T_\lambda = \frac{8\pi^2 m}{3h(2J+1)} \left\{ \frac{(n^2+2)^2}{9n} \right\} (2\lambda + 1) \sum_t (2t+1) B_t \Xi^2(t, \lambda) \tag{24.7}$$

Substituting $\nu = c\sigma$ and eq. (24.7) into eq. (24.6) gives

$$P_{ED} = \frac{8\pi^2 mc\sigma}{3h(2J+1)} \left\{ \frac{(n^2+2)^2}{9n} \right\} \sum_{\lambda=2,4,6} \Omega_\lambda (\psi J \| U^{(\lambda)} \| \psi' J')^2 \tag{24.8}$$

where $\Omega_\lambda = (2\lambda + 1)\Sigma_t (2t+1) B_t \Xi^2(t, \lambda)$ (Axe, 1963), and in terms of $\bar{F}^2$, eq. (24.5),

$$\bar{F}^2 = e^2 \sum_{\lambda=2,4,6} \Omega_\lambda (\psi J \| U^{(\lambda)} \| \psi' J')^2 \tag{24.9}$$

The matrix elements of eq. (24.8) are calculated in the LS basis using the relation (Judd, 1962),

$$\begin{aligned} &(f^N \alpha S L J \| U^{(\lambda)} \| f^N \alpha' S' L' J') \\ &= \delta(S, S')(-1)^{S+L'+J+\lambda} [(2J+1)(2J'+1)]^{1/2} \begin{Bmatrix} J & J' & \lambda \\ L' & L & S \end{Bmatrix} (f^N \alpha S L \| U^{(\lambda)} \| f^N \alpha' S' L'). \end{aligned} \tag{24.10}$$

Selection rules imposed by the nature of the mechanism assumed are discussed by Ofelt (1962). The reduced matrix elements on the right side of eq. (24.10) have been tabulated by Nielson and Koster (1963). The matrix elements as computed must be transformed from the LS basis to intermediate coupling before being squared and substituted into eq. (24.8).

The intermediate-coupling eigenvectors, $|f^N \psi J\rangle$, are expressed in terms of LS basis states, $|f^N \alpha S L J\rangle$, by:

$$|f^N \psi J\rangle = \sum_{\alpha, S, L} c(\alpha, S, L) |f^N \alpha S L J\rangle$$

where $c(\alpha, S, L)$ are the numerical coefficients resulting from the simultaneous diagonalization of the terms indicated in eq. (24.1).

3.5. *Magnetic dipole transitions*

Following the results of Condon and Shortley (1957), the magnetic dipole operator is given as $M = (-e/2mc)\Sigma_i(L_i + 2S_i)$. The matrix elements of the operator $\bar{M}^2$ in eq. (24.5) can then be written,

$$\bar{M}^2 = (e^2/4m^2c^2)(\psi J\|L + 2S\|\psi' J')^2. \tag{24.11}$$

The non-zero matrix elements will be those diagonal in the quantum numbers α, S, and L. The selection rule on J, $\Delta J = 0, \pm 1$, restricts consideration to three cases,

$$(1)\quad J' = J \qquad (\alpha SLJ\|L + 2S\|\alpha SLJ') = g\hbar[J(J+1)(2J+1)]^{1/2} \tag{24.12}$$

$$\text{where } g = 1 + \frac{J(J+1) + S(S+1) - L(L+1)}{2J(J+1)}$$

$$(2)\quad J' = J - 1 \qquad (\alpha SLJ\|L + 2S\|\alpha SLJ - 1)$$
$$= \hbar\left[\frac{(S+L+J+1)(S+L+1-J)(J+S-L)(J+L-S)}{4J}\right]^{1/2} \tag{24.13}$$

$$(3)\quad J' = J + 1 \qquad (\alpha SLJ\|L + 2S\|\alpha SLJ + 1)$$
$$= \hbar\left[\frac{(S+L+J+2)(S+J+1-L)(L+J+1-S)(S+L-J)}{4(J+1)}\right]^{1/2}. \tag{24.14}$$

The matrix elements calculated in eqs. (24.12–24.14) must be transformed into the intermediate coupling scheme before computation of the magnetic dipole contribution represented by eq. (24.11).

Values of the quantity $P' > 0.015 \times 10^{-8}$ where $P_{MD} = P'n$ have been calculated for all of the trivalent lanthanide ions based on eigenvectors derived from energy level schemes for R^{3+}(aquo) (Carnall et al., 1968a). The principal magnetic dipole transitions in the absorption spectra of the 3+ lanthanides are identified in table 24.3.

3.6. *Comparison of experimental and calculated oscillator strengths*

The most complete oscillator strength data for lanthanide solution absorption spectra have been given by Stewart (1959) and by Carnall et al. (1968a). The results obtained when the parameters of eq. (24.8) are determined by a least squares fitting procedure to the data for a given R^{3+} ion, corrected for P_{MD} where appropriate, are summarized in table 24.4. As was pointed out in section 3.4, the parameterization in terms of Ω_λ lends itself readily to discussion of both absorption and fluorescence spectra, and has been used almost exclusively in describing data obtained in crystals, ch. 35. It serves no purpose to continue to preserve several different parameterizations. We adopt here the use of Ω_λ.

TABLE 24.3.
Oscillator strengths (P') of the principal magnetic dipole transitions in the absorption spectra of the 3+ lanthanides in solution.

	Excited[a] state	E^{b}_{calc} (cm^{-1})	$P' \times 10^{8}$ [b,c]		Excited[a] state	E^{b}_{calc} (cm^{-1})	$P' \times 10^{8}$ [b,c]
Pr^{3+}	$^3H_5$	2322	9.76	Tb^{3+}	$^7F_5$	2112	12.11
					$^7F_4$	26425	5.03
Nd^{3+}	$^4I_{11/2}$	2007	14.11		$^5F_5$	34927	1.87
Pm^{3+}	$^5I_5$	1577	16.36	Dy^{3+}	$^6H_{13/2}$	3506	22.68
					$^4I_{15/2}$	22293	5.95
Sm^{3+}	$^6H_{7/2}$	1080	17.51				
	$^4G_{5/2}$	17924	1.76	Ho^{3+}	$^5I_7$	5116	29.47
					$^3K_8$	21308	6.39
Eu^{3+}	$^7F_1$	350	17.73				
	$^5D_1$	19026	1.62	Er^{3+}	$^4I_{13/2}$	6610	30.82
	$^5F_1$	33429	2.16		$^2K_{15/2}$	27801	3.69
Gd^{3+}	$^6P_{7/2}$	32224	4.13	Tm^{3+}	$^3H_5$	8390	27.25
	$^6P_{5/2}$	32766	2.33				
				Yb^{3+}	$^2F_{3/2}$	10400	17.76

[a]Principal L–S state. [b]Calculated using parameters given in table 24.4. [c]Results are given for $P' > 1.5 \times 10^{-8}$ where $P_{MD} = P'n$ and $n = 1.33$ for dilute acid solutions.

TABLE 24.4.
Values of the Judd–Ofelt intensity parameters, Ω_λ, for the lanthanides in dilute acid solution[a].

R^{3+}	$\Omega_2(cm^2)$	$\Omega_4(cm^2)$	$\Omega_6(cm^2)$
Pr[b]	32.6×10^{-20}	5.7×10^{-20}	32.0×10^{-20}
Nd	0.93	5.00	7.91
Pm	2.80	2.52	4.20
Sm	0.91	4.13	2.70
Eu[c]	1.46	6.66	5.40
Gd	2.56	4.70	4.73
Tb	.004	7.19	3.45
Dy	1.50	3.44	3.46
Ho	0.36	3.14	3.07
Er	1.59	1.95	1.90
Tm	0.80	2.08	1.86
Yb	—	1.65	1.65

[a]Original results from Carnall et al. (1968b). [b]From Carnall et al. (1965). [c]For purposes of comparison with other members of the series, the parameters for Eu^{3+} were increased by a factor of 1.546. See Carnall et al. (1968b).

Conversion factors for the various parameterizations of the electric dipole oscillator strength are:

(a) $\mathcal{T}_\lambda(\text{cm})$ (Carnall et al., 1965) $= (2J+1)cT_\lambda$ (Judd, 1962)

(b) $\Omega_\lambda(\text{cm}^2)$ (Axe, 1963) $= \left[\frac{8\pi^2 mc}{3h}\right]^{-1} \mathcal{T}_\lambda = (1.086\times 10^{11})^{-1}\mathcal{T}_\lambda$

Use of the parameters in table 24.4 is illustrated by the comparison of calculated and observed data for Tb^{3+}(aquo) shown in table 24.5. It is evident that large variations in intensities between different groups are reproduced by the theory. Typically, several excited states are encompassed by a single complex absorption envelope, and the matrix elements of $U^{(\lambda)}$ are summed over these states. The energy in this case becomes that of the center of gravity of the envelope. While many transitions are weak, as judged from the magnitude of the corresponding matrix elements, the few transitions principally responsible for the intensity of a given band can be readily identified. At an earlier stage, this fact was the basis for the extensive use of intensity correlations as a means of making energy level assignments to solution spectra. It resulted in the first successful effort to derive a consistent set of free-ion energy level parameters including effective operators of configuration interaction for the whole series of trivalent lanthanide ions, as shown in table 24.2 (Carnall et al., 1968a).

TABLE 24.5.
Observed and calculated oscillator strengths for Tb^{3+}(aquo).

SLJ[a]	Spectral range[b] $(\text{cm}^{-1})\times 10^{-3}$	$P\times 10^6$ Expt.	Calc.[c]
$^7F_5$	2.112	—	0.16[d] 1.04[e]
$^7F_4$	3.370	—	1.54
$^7F_3$	4.344	—	1.35
$^7F_2$	5.028	—	0.98
$^7F_1$	5.481	—	0.70
$^7F_0$	5.703	—	0.28
$^5D_4$	20–21.2	0.52	0.21
$^5D_3, {}^5G_6, {}^5L_{10}$	25.9–27.6	8.46	0.07[d] 7.61[e]
$^5G_5, {}^5D_2, {}^5G_4, {}^5L_9$	27.6–28.95	7.46	7.61
$^5G_3, {}^5L_8, {}^5L_7, {}^5L_6, {}^5G_2$	28.95–30.2	3.04	4.03
$^5D_1$	30.4–30.9	0.37	0.32
$^5D_0, {}^5H_7$	30.95–32.0	2.02	1.85
$^5H_6$	32.5–33.5	1.20	1.41
$^5H_5$	33.6–34.1	0.18	0.47
$^5H_4, {}^5F_5, {}^5H_3, {}^5I_8, {}^5F_4$	34.4–35.8	5.05	5.32

[a]The principal L–S component(s) is shown. [b]The calculated free-ion energy of the state is shown for the levels of the ^{7}F-multiplet. For the observed bands, the range encompassed by the band group is noted. [c]Calculated using the parameters of table 24.4. [d]Calculated magnetic-dipole strength. [e]Calculated electric-dipole strength.

3.7. *Use of intensity parameters to estimate oscillator strengths of infrared transitions*

In addition to the use of intensity correlations as an aid in making energy level assignments, the parameters given in table 24.4 can be used to predict the oscillator strength associated with transitions that cannot be observed in aqueous solution. The results given for Tb^{3+}(aquo), table 24.5, illustrate this by the inclusion of calculated intensities associated with bands in the infrared region. In many cases such bands will be intense compared to those observed in the visible region and can be observed if an appropriate solvent is used. See section 2.2. While the energy of the center of gravity (free-ion level energy) is known for these infrared transitions, the band width, the complex structure, and the associated intensities are not known.

In order to emphasize the relative intensities of the infrared bands in R^{3+} spectra, a computer program was developed to calculate the molar absorptivity of a Gaussian curve of specified base energy interval, width at half-height, and area. The half-width was arbitrarily set at 50 cm^{-1}. The energy interval was taken as that observed for the corresponding R^{3+} bands observed in $LiNO_3$–KNO_3 eutectic at 150°C (Carnall et al., 1965), where possible. Otherwise an arbitrary scale based on the energy of the transition was used. The results are included as dashed line curves in figs. 24.4–24.12. The parameters used to compute the band areas for Pr^{3+} were those for Pr^{3+} in $LiNO_3$-KNO_3 eutectic (Carnall et al., 1965). For Pr^{3+} the band at ~5000 cm^{-1}, fig. 24.4, encompasses two levels.

3.8. *Hypersensitive transitions*

The fact that the intensities of certain bands in the solution spectra of the trivalent lanthanides are remarkably sensitive to changes in the environment has been known for many years. For example, in an investigation of the effects of nitrate ion concentration on the spectra of a number of lanthanides, Selwood (1930) showed that relative to the other bands, one or two bands in the spectra of Nd^{3+}, Eu^{3+}, Ho^{3+} and Er^{3+} exhibited greatly increased intensities at high nitrate concentration compared to dilute solution. Such bands have subsequently been labeled "hypersensitive". These transitions follow electric quadrupole selection rules, $\Delta J \leqslant \pm 2$. Increases in oscillator strength by more than a factor of 3 are observed in some environments.

With the development of the Judd–Ofelt Theory, Judd (1962) pointed out that of the three parameters, T_λ, eq. (24.6), T_2 most closely monitors changes in the environment, and that hypersensitivity was strongly correlated with those transitions having large matrix elements of $U^{(2)}$. Jørgensen and Judd (1964) examined some of the potential mechanisms for hypersensitive transitions, discarding the possibility that they could exhibit electric quadrupole character. It was suggested that the origin might lie in an inhomogeneous dielectric. Subsequently Judd (1966b) pointed out that symmetry arguments could be introduced to classify site symmetries in which hypersensitivity might be in-

duced. Peacock (1975) has reviewed some of the arguments but no definitive interpretation has been offered. Hendrie et al. (1976) have discussed hypersensitivity in terms of a correlation which they found between oscillator strength and ligand basicity. The term "hypersensitive transitions" as used by the above authors and by Jørgensen and Judd (1964) refers to a limited clearly defined set of experimental observations. Unfortunately the term is occasionally used by other authors in a very broad, ill-defined manner.

4. Fluorescence spectra in solution

The existence of characteristic fluorescence spectra in aqueous solutions of the lanthanides was extensively reported in the early 1930's. Much of the data was qualitative, but a number of transitions were identified, and recent characterization of the energy level schemes involved makes possible considerable additional interpretation. The analytical potential of the fluorescence spectra was recognized and exploited at an early stage. More recent interest in fluorescence in solution derives in part from the ability to determine lifetimes of the fluorescing states and to use this as a basis for exploring excited state relaxation and energy transfer mechanisms. With laser excitation, micro to nanosecond lifetimes can be readily measured. Thus in contrast to absorption spectra where only shifts in band energy or changes in band shape can be correlated with changes in the ionic environment, fluorescence spectra investigations can also yield characteristic lifetimes of the relaxing states. It will be shown that such measurements provide a highly sensitive monitor of changing environment.

The forced–electric and magnetic dipole mechanisms discussed relative to the absorption of radiation are also primarily responsible for the radiative relaxation of excited states. Non-radiative relaxation, which usually competes strongly with the radiative mode, is under active investigation, and several different mechanisms have been discussed.

4.1. *Historical development*

It was pointed out at an early stage that those lanthanides that fluoresced in solid compounds at room temperature, also exhibited fluorescence in solution at approximately the same energy and with the same relative intensities (Tomaschek and Deutschbein, 1933); Deutschbein and Tomaschek, 1937). Maximum fluorescence yield was observed at the center of the series, Eu^{3+}, Gd^{3+}, Tb^{3+}, with intensity dropping rapidly at Sm^{3+} and Dy^{3+} (Tomaschek and Mehnert, 1937; Gobrecht, 1938), and transitions between a number of well characterized excited states and components of the ground term multiplet were identified (Zaidel, 1937). The particular sensitivity of both the intensity and energy of fluorescing transitions in Eu^{3+} to changes in the ionic environment was discussed by Tomaschek (1939, 1942). Deutschbein and Tomaschek (1937) attributed the

existence of structure in the weak $^5D_0 \rightarrow {}^5F_0$ transition in Eu^{3+} to the presence of multiple species of Eu^{3+}.

The analytical aspects of fluorescence spectra in lanthanide solutions were exploited by a number of groups to detect Ce^{3+}, Sm^{3+}, Gd^{3+}, Tb^{3+}, and Dy^{3+} as impurities in solutions of other lanthanides (Gobrecht and Tomaschek, 1937; Zaidel et al., 1938; Zaidel and Lavionov, 1939, 1943). Fassel and Heidel (1954) used the intense fluorescence of Tb^{3+}(aquo) as the basis for developing quantitative analytical procedures.

4.2. *Relaxation of excited states in solution. General considerations*

A great deal of progress has been made in analyzing the mechanisms of excited state relaxation of lanthanides in crystal hosts, ch. 35, and these concepts have also diffused into the literature on solutions. Two modes of relaxation can be recognized: radiative and non-radiative processes. Axe (1963) addressed the problem of expressing the radiative process in quantitative terms using the Judd–Ofelt theory. Non-radiative relaxation was already being formulated in terms of multiphonon processes in the early 1960's (Barasch and Dieke, 1965; Riseberg and Moos, 1968). Such processes become less probable as the energy gap between an excited state and the next lower energy state increases.

4.3. *Radiative relaxation*

In treating the fluorescence process, the Einstein coefficient, eq. (24.4) is used directly to express the rate of relaxation of an excited state (ψJ) to a particular final state $(\psi' J')$. Following Axe (1963), the counterpart of eq. (24.5) becomes

$$A(\psi J, \psi' J') = \frac{64\pi^4\sigma^3}{3h(2J+1)}[\chi' \bar{F}^2 + n^3 \bar{M}^2] \tag{24.15}$$

where $\sigma(\mathrm{cm}^{-1})$ represents the energy gap between states (ψJ) and $(\psi' J')$, $\chi' = n(n^2+2)^2/9$, and n is the refractive index of the medium. As in the absorption process, there is an implicit assumption that all (crystal-field) components of the initial state are equally populated. In principal, if fluorescence can be detected, the lifetime of the state is long compared to the rate at which it is populated in the excitation process, so thermal equilibrium at the temperature of the system can be achieved prior to emission.

The matrix elements of the electric and magnetic dipole operators, $\bar{F}^2$ and $\bar{M}^2$, are identical to those in eq. (24.9) and eq. (24.11), respectively. However, the form of the refractive index correction in eq. (24.15) is not the same as for the absorption process, eq. (24.5). Equation (24.15) can be evaluated using parameters Ω_λ established from measurement of the absorption spectrum of the lanthanide ion in a solution identical to that studied in fluorescence.

Since excited state relaxation generally involves transitions to several lower-lying states, we define a total radiative relaxation rate, $A_T(\psi J)$

$$A_T(\psi J) = \sum_{\psi' J'} A(\psi J, \psi' J') \tag{24.16}$$

where the sum runs over all states lower in energy than the fluorescing state.

It is useful to define in addition the radiative branching ratio, β_R, from the relaxing state (ψJ) to a particular final state ($\psi' J'$):

$$\beta_R(\psi J, \psi' J') = \frac{A(\psi J, \psi' J')}{A_T(\psi J)} \tag{24.17}$$

and the radiative lifetime of a state

$$\tau_R(\psi J) = [A_T(\psi J)]^{-1} \tag{24.18}$$

The principal fluorescing states in aqueous solutions containing the lanthanide ions were identified in experimental investigations undertaken in the 1930's. Toward the beginning and end of the series, lifetimes were too short for fluorescence to be detected, but lines characteristic of Sm^{3+}, Eu^{3+}, Gd^{3+}, Tb^{3+}, and Dy^{3+} were discerned. Since the parameters, Ω_λ, have been determined for all the lanthanides in dilute acid solution, table 24.4, the total radiative lifetime of any excited state can be readily computed. The results shown in table 24.6 are in most cases for the resonance level which is the excited state which has the largest energy gap to the next lower state. As will be discussed in section 4.5, non-radiative relaxation is at a minimum in Gd^{3+}(aquo) so that the measured lifetime of Gd^{3+} in H_2SO_4 ($\tau = \sim 2$ msec) (Kondrat'eva and Lazeeva, 1960), compares well with the calculated radiative lifetime of the state.

4.4. *Non-radiative relaxation. General considerations*

Although much is known about the non-radiative mechanisms of relaxation of fluorescing states in aqueous solution, there is presently no quantitative theory. Consequently, the symbolism used here follows that introduced in the study of the solid state where the theory has undergone more extensive development.

Since in the usual case both radiative and non-radiative processes operate to relax an excited state, we can express the total fluorescence lifetime of the state as

$$(\tau_T)^{-1} = A_T(\psi J) + W_T(\psi J) \tag{24.19}$$

TABLE 24.6.
Calculated radiative lifetimes of excited states of R^{3+}(aquo)[a].

Excited state[b]	Nd $^4F_{3/2}$	Pm $^5F_1$	Sm $^4G_{5/2}$	Eu $^5D_0$	Gd $^6P_{7/2}$	Tb $^5D_4$	Dy $^4F_{9/2}$	Ho $^5S_2$	Er $^4S_{3/2}$
Energy of excited state (cm^{-1})	11460	12400	17900	17277	32200	20500	21100	18500	18350
$\tau_R(\psi J)$ (msec)	0.42	0.65	6.26	9.67	10.9	9.02	1.85	0.37	0.66

[a]The total radiative (electric and magnetic dipole) lifetime, eq. (24.18), is given. The electric-dipole contribution was calculated from eq. (24.9) using values of Ω_λ given in table 24.4. [b]Major component of the eigenvector is indicated.

where A_T is the radiative rate and $W_T(\psi J)$ is the sum of the rates of the various non-radiative processes. In crystalline hosts it has been shown that the dependence of the non-radiative rate on the energy gap (ΔE) between the excited level and the next lower-lying level is of the form:

$$W_T = Ce^{\alpha \Delta E} \tag{24.20}$$

where C and α are constants characteristic of a particular crystal (Riseberg and Moos, 1968). The relaxation mechanism is interpreted as a multiphonon process which becomes less probable as the number of phonons that must be simultaneously excited to conserve energy increases.

4.5. *Multiphonon-like processes in solution*

Investigations of the enhancement of the fluorescence yield of lanthanide ions in D_2O compared to H_2O provided the basis for extending the concepts of multiphonon relaxation to aqueous solutions. The H_2O–D_2O system was selected for fluorescence enhancement experiments since the substitution of D_2O for H_2O has been shown to exert no change in the absorption spectrum of a lanthanide ion (Kropp and Windsor, 1965; Gallagher, 1965; Borkowski et al., 1965). Such spectra are known to be sensitive to the effects of complexing by many different anionic species even in very dilute solutions (Kondrat'eva, 1960; Kondrat'eva and Lazeeva, 1960; Gallagher, 1964). Complexing measurably influences the radiative lifetime of the fluorescence. In contrast to the behavior reported for lanthanide ions, the spectra of a number of transition metal ions were displaced toward higher energies when H_2O was substituted for D_2O. The necessity for the isotopic substitution to take place in the inner coordination sphere to achieve an effect was noted (Halpern and Harkness, 1959; Bigeleisen, 1960).

In their pioneering work, Kropp and Windsor (1963, 1965, 1966) pointed out that the ratio of the intensity of fluorescence of a given R^{3+} state in D_2O to that of the same state in H_2O bore an inverse relation to the energy gap. This is illustrated in table 24.7 where the original data has been supplemented with similar results obtained later by others.

Kropp and Windsor (1965) concluded that quenching of fluorescence in aqueous solution occurred via −OH coupled modes and that the rate was proportional to the number of such modes associated with the lanthanide ions. Gallagher (1965) found that the experimentally observed decay curves of the Eu^{3+}(aquo) $^5D_0 \rightarrow {}^7F_1$ emission as a function of increasing H_2O concentration in D_2O could be resolved into the sum of two exponentials. The results were interpreted as indicating that the introduction of a single OH group into the inner coordination sphere of Eu^{3+} was sufficient to reduce the fluorescence lifetime of the $^5D_0$ state from 3.9 to 0.12 msec. Heller (1966) used the relative intensity of fluorescence in D_2O to H_2O, (I_D/I_H) as a function of [H_2O] at low concentrations in D_2O to show that the rate determining step in the quenching of lanthanide fluorescence in H_2O was associated with transfer of energy to a single vibrational mode (OH) which is subsequently excited to high vibrational states. This

TABLE 24.7.
Fluorescence intensities and lifetimes of lanthanide excited states in H_2O and D_2O.

	I_D/I_H[a]	ΔE[b] (cm^{-1})	Lifetime[c] (msec) τ_{H_2O}	τ_{D_2O}
Gd^{3+}	1.0 ± 0.2	32100	2[d](2.3)[e]	
Tb^{3+}	7.8 ± 0.8	14700	.39(.48)[f]	3.3(4.0)[f]
Eu^{3+}	18.0 ± 1.8	12300	.10(.12)[f]	1.9(4.0)[f]
Dy^{3+}	12 ± 3	7800	$\leq$.003[f](.0023)[e]	.06[f](.038)[e]
Sm^{3+}	12 ± 6	7500	$\leq$.003[f](.0022)[e]	.075[f](.053)[e]

[a]Solutions were 0.1 M $R(NO_3)_3$ in H_2O or D_2O, and the intensity of fluorescence in D_2O was normalized to unity in H_2O in each case. [b]ΔE is the difference in energy between the excited (resonance) level and the next lower energy level. [c]The results are from Kropp and Windsor (1965) except as indicated. [d]Kondrat'eva and Lazeeva (1960). [e]Stein and Würzberg (1975). [f]Kazanskaya and Sveshnikova (1970).

was contrasted to possible alternative processes which would have involved either several different modes of a simple molecule or energy transfer to vibrational modes of several molecules. Haas and Stein (1971a) interpreted structure observed in Gd^{3+}(aquo) as vibronic satellites due to coupling −OH or −OD to the 312 nm fluorescing state.

As pointed out by Heller (1966), the changes in the vibrational quantum numbers necessary to bridge the energy gaps already cited, using ν_1 (OH) = 3405 cm^{-1} (O–H fundamental) and ν_1 (OD) = 2520 cm^{-1} (Hornig et al., 1958), are as follows:

$\Delta E/\nu_1$	OH	OD
Gd^{3+}	10	13
Tb^{3+}	5	6
Eu^{3+}	4	5
Dy^{3+}	3	4
Sm^{3+}	3	4

Since the lifetimes associated with Sm^{3+}(aquo) and Dy^{3+}(aquo) were short, Stein and Würzburg (1975) give ~2 μsec in each case, and other ions with $\Delta E < 6500\ cm^{-1}$ (Pr^{3+}, Nd^{3+}, Ho^{3+}, Er^{3+}) barely fluoresce in H_2O or D_2O (Ermolaev and Sveshnikova, 1970), the results in solution appear to be comparable to those pointed out by Barasch and Dieke (1965) as characteristic of the $LaCl_3$ host. Fluorescence at room temperature was not observed from an excited state if the energy gap to the next lower level were $< 1000\ cm^{-1}$. Since the phonon density of states cuts off at ~260 cm^{-1} in $LaCl_3$, this gap corresponds to an ~3 phonon emission process.

Similarly, at the other extreme, Kropp and Windsor (1965), pointed out that the gap in Gd^{3+} is so large that multiphonon-like relaxation is already a very high order (and thus low probability) process when the coordinating group is OH.

Substitution of D_2O therefore has no further detectable effect. Their computed value of τ_R based on integrated absorption measurements was 5.4 msec compared to a measured value of ~2 msec (Kondrat'eva and Lazeeva, 1960), and they concluded that non-radiative processes other than those associated with OH-modes must contribute to this relaxation process. The results in table 24.6 based on theory in section 3.4 suggest that the emission is consistent with a purely radiative relaxation mechanism.

4.6. *Other non-radiative relaxation mechanisms in solution*

Fluorescence yield studies have shown that mechanisms other than multiphonon-like processes can play an important part in the non-radiative relaxation of some states. For example, Kropp and Windsor (1965) pointed out that for $Eu(NO_3)_3$ in CH_3OH, only about one-half of the energy associated with the excited $^5D_1$ state is transferred to the lower $^5D_0$ state. The remainder is transferred to ground by other processes. This fast non-radiative decay of the $^5D_1$ state also accounts for the temperature dependent decrease in the lifetime of the $^5D_0$ state, since at higher temperature some thermal excitation to the $^5D_1$ from the $^5D_0$ state occurs, and the very rapid non-radiative decay associated with the $^5D_1$ state aids in the deactivation of the $^5D_0$ state (Kropp and Dawson, 1966).

It may be noted in passing that no quenching effect on fluorescence was attributable to dissolved O_2 in aqueous solution nor to the presence of I^- (Kropp and Windsor, 1965), but ion-ion interaction may be a mode of relaxation depending upon the energy level scheme. It can operate to deactivate the $^5D_3$ state in Tb^{3+} directly to the ^7F-multiplet (Goldschmidt et al., 1975). Stein and Würzberg (1975) have also pointed out cases where radiationless relaxation occurs by modes other than those associated with multiphonon-like processes and have made approximate calculations.

4.7. *Theoretical models for radiationless relaxation of excited states in solution*

In their discussion of the rates of non-radiative energy transfer in molecules (Robinson and Frosch, 1963) pointed out that large isotope effects may arise in solution where significant amounts of electronic energy are converted into vibrational modes in the system. This motivated some of the earlier investigations of lanthanides in H_2O–D_2O systems. More recently Siebrand (1967) carried out an extensive investigation of the Franck-Condon factors that are part of the Robinson and Frosch theory and obtained the expression:

$$W_{AB} = (2\pi\rho_E/\hbar)J^2F \tag{24.21}$$

where W is the radiationless transition probability per unit time, ρ_E is the density of final states within which vibrational deactivation is rapid relative to any electronic relaxation, J is Siebrand's electronic transition matrix element between the initial (A) and final (B) states, and F is the Franck-Condon factor. If it is assumed that changes in the radiationless rate constant are due primarily to F,

that is, that ρ_E and J are effectively constant, then it can be shown that $F(E)$, for small values of the energy gap E, varies essentially exponentially with the order of the vibrational process (Henry and Kasha, 1968). Bodunov and Sveshnikova (1974) reached the same conclusion with respect to the exponential dependence of W_{AB} on the order of the process based on modeling the intramolecular vibrations of H_2O by Morse oscillators. Thus for R^{3+}(aquo) ions, a multiphonon-like process similar in form to that given by Riseberg and Moos (1968) for crystals, eq. (24.20), is an important relaxation mode.

Haas and Stein (1972) using the Siebrand model and spectroscopic results for Gd^{3+}(aquo), calculated non-radiative relaxation rates for different order processes, and compared them with rates determined experimentally for several lanthanide ions. There was good correlation in the magnitude of change with the order of the process, but quantitative agreement was not achieved. Sveshnikova and Ermolaev (1971) used a dipole-dipole interaction approximation to compute rate constants for non-radiative relaxation, but the correlation with experimental results was poor.

Further development of theoretical models that can be used to interpret non-radiative relaxation processes in solution in greater detail is certain to be fruitful. At present a basic result obtained is that multiphonon-like processes of order greater than 5 or 6 cannot compete effectively with radiative modes of relaxation.

4.8. *Hydration and coordination numbers of* R^{3+}(aquo). *Application of fluorescence lifetime measurements*

When a cation such as R^{3+} is thrust into aqueous solution, the bulk structure is modified and two different regions about the ion can be arbitrarily defined. Region A: The H_2O molecules in the direct vicinity of the ion constitute the primary (inner) coordination sphere, and there is a kinetic distinction between these molecules and those in the bulk solvent (Hindman and Sullivan, 1971). The number of molecules in this sphere is the coordination number. Region B: Extending beyond the first region is a second (outer) shell which contains H_2O molecules that are not in contact with the central ion. They interact with the inner sphere, and consequently this region has a structure that is different from that of the bulk solvent. The extent of the outer shell is defined by the measurable effect it has on processes occurring in solution (Rosseinsky, 1965; Entelis and Tiger, 1976).

As Spedding et al. (1974) pointed out, the increase in charge density on the surface of a lanthanide ion as the ionic radius decreases, results in an increase in the total extent of hydration (Regions A and B) with atomic number. This is consistent with trends in conductivity and viscosity measurements. Choppin and Graffeo (1965) estimated hydration numbers from conductance data obtaining 12.8 ± 0.1 for La^{3+}–Nd^{3+}, 13.1–13.4 for Sm^{3+}–Gd^{3+}, and 13.9 ± 0.1 for $Dy^{3+} - Yb^{3+}$.

Since the coordination number of a lanthanide ion can only be accurately defined with respect to a crystal lattice, the concept must remain approximate

when applied to solutions. Nevertheless, a number of estimates have been made, and conflicting viewpoints exist as to whether or not there is a change in coordination number across the series. Undoubtedly part of the problem lies in the interpretation given to different experiments. Karraker (1970) found the spectra of Nd^{3+} in dilute solutions and in crystalline $Nd(BrO_3)_3 \cdot 9H_2O$ to be very similar and took this as evidence supported by other measurements for the coordination number of 9 in Nd^{3+}(aquo). Geier et al. (1969) and Reuben and Fiat (1969a,b) interpreted their spectroscopic and NMR results, respectively, as indicating that the coordination number (probably 9), is constant in dilute solution. Hinchley and Cobble (1970) found no evidence for a change in coordination number over the series from their correlation between ionic entropy and radius. This was in contrast to the conclusions of a similar study by Bertha and Choppin (1969).

More recently Spedding et al. (1974), Habenschuss and Spedding (1974), and Rard and Spedding (1974) have summarized evidence based on X-ray as well as a number of different thermodynamic studies supporting the position that there is a change in coordination number of R^{3+}(aquo) across the series. The hydrated lanthanide ions in dilute solution exhibit a coordination number of 9 from La^{3+} to Nd^{3+}, and 8 from Tb^{3+} to Yb^{3+}. The intermediate ions presumably exhibit a mixture of these coordination numbers.

Insight into the nature of the coordination sphere in R^{3+}(aquo) was obtained by Kropp and Windsor (1967) from fluorescence lifetime studies. The addition of acetate ion (Ac^-) to solutions of $EuCl_3$ or $TbCl_3$ in H_2O increases both the total fluorescence intensity and the lifetime of the fluorescing states. In contrast, the lifetimes decrease in D_2O with increasing [Ac^-]. Comparison of the rates of relaxation in H_2O and D_2O made it possible to determine the radiative rate constant for fluorescence emission which could be related to the fraction of the hydration shell not replaced by Ac^-, m/m_s, as a function of [Ac^-]. The variation of m/m_s with [Ac^-] was compared to data on Ac^- complexing of R^{3+} obtained by Sonesson (1958), and this resulted in the relationship $m_s/n = 6$ where m_s is the hydration number for pure H_2O and n is the number of H_2O molecules replaced by each Ac^-. If n is assumed to be 2, the resulting hydration number of 12 is near the value estimated by Choppin and Graffeo (1965) from conductance measurements. A similar experiment in which the fluorescence lifetime of the $^5D_0$ state of Eu^{3+} was monitored in H_2O–CH_3CN mixtures was interpreted by Haas and Stein (1971b) in terms of a step-wise quenching mechanism. By comparing the bimolecular rate constant for quenching due to one molecule of H_2O, ($1100\ sec^{-1}$) as determined from quantum yield and total fluorescence lifetime data, with the total quenching rate constant in aqueous solution ($9800\ sec^{-1}$), it appears that formally, only 9 molecules of H_2O participate in the quenching process in aqueous solution. This is close to the expected coordination number for Eu^{3+}(aquo), but should be taken as the effective number for the $^5D_0$ excited state.

5. Oxidation states of the lanthanides observed in dilute aqueous solution

5.1. *Standard oxidation potentials*

Standard oxidation potentials referred to the normal hydrogen electrode ($E°$) for the divalent and trivalent lanthanide aquo ions are given in table 24.8 based primarily on the selected experimental results compiled by Charlot et al. (1971) and the systematic correlations summarized by Nugent (1975). Only Eu^{2+} and Yb^{2+} can persist for times of the order of minutes to hours in dilute acid solution, and can be readily produced by reduction of the trivalent ionic species (Laitinen and Taebel, 1941; Laitinen, 1942; Christensen et al., 1973). The value of $E° = -0.43$ V for the Eu(II–III) couple quoted in many previous compilations was obtained using both potentiometric and polarographic techniques. However, in a reevaluation of the solution thermodynamic properties of europium, Morss and Haug (1973) recommended the value $E° = -0.35$ V.

The III–IV potentials of both Pr and Tb were placed in the +(3.3–3.4) V range by Nugent et al. (1973) based on correlations between $E°$ and observed spectroscopic properties, as well as by use of Jørgensen's refined electron spin-pairing theory. However, the reported oxidation of Pr III to Pr IV by the OH radical during pulse radiolysis experiments, section 5.2, suggests that the esti-

TABLE 24.8.
Standard oxidation potentials (relative to the standard hydrogen electrode).[a]

	II–III Potential[b] $E°_{298\,K}$ (volts)	III–IV Potential[b] $E°_{298\,K}$ (volts)
Ce	−3.2	1.70[c], 1.74
Pr	−2.7	ca. 2.9[d], 3.4
Nd	−2.6	4.6
Pm	−2.6	4.9
Sm	−1.56[e]	5.2
Eu	−0.35[e]	6.4
Gd	−3.9	7.9
Tb	−3.7	3.3
Dy	−2.6	5.0
Ho	−2.9	6.2
Er	−3.1	6.1
Tm	−2.3	6.1
Yb	−1.15[f]	7.1

[a]The 1969 IUPAC sign convention is used. The greater the positive potential, the more stable the reduced form. [b]Except where specifically cited, the values shown were calculated or derived from spectrophotometric data by Nugent et al. (1973). [c]Charlot et al. (1971). [d]Eyring et al. (1952). [e]Morss and Haug (1973). [f]Laitinen (1942).

mated (III–IV) potentials previously cited may be too high. At pH ~6, the oxidizing potential of the OH radical would be estimated to be only ~2.4 V (Henglein, 1974). Jørgensen (1976) has pointed out that the calculated III–IV potentials refer to the formation of a hypothetical highly acid R(IV) aquo ion. It can be argued that at pH $\geqslant$5, a much more stable species $R(OH)^{3+}$ or $R(OH)_z^{2+}$ may be formed. In this case the $E°$ value would be less positive than that predicted. Results of pulse radiolysis experiments with Gd^{3+} and Ho^{3+} quoted in section 5.2 indicate that the II–III oxidation potentials of these ions lie in the range ca. −(2.3–2.8 V).

5.2. *Production of unusual oxidation states in solution by pulse radiolysis*

One of the most powerful techniques of radiation chemistry is pulse radiolysis. Accelerators capable of producing electron pulses on the micro to nanosecond time scale are now in wide-spread use and provide a unique means for studying oxidation-reduction reactions in aqueous solution. The interaction of high energy electrons with H_2O results in the net ionization reaction $2H_2O \rightarrow H_3O^+ + OH + e^-_{aq}$ which is complete in $\approx 10^{-11}$ sec. Since the hydrated electron, e^-_{aq}, and the OH-radical represent, respectively, an extremely strong reducing/oxidizing agent, unusual reactions can be induced. By the addition of a suitable scavenger to the system, it is possible to selectively study the reaction of either e^-_{aq} or OH with solute species. For example, H_2 rapidly converts the OH- radical to e^-_{aq} by the reactions $OH + H_2 \rightarrow H_2O + H$, $H + OH^- \rightleftarrows e^-_{aq}$.

The potentials associated with the redox reactions of R^{3+}(aquo) span a wide range, table 24.8, and characteristic absorption spectra are obtained for the various oxidation states. As a consequence, this represents an interesting area for pulse radiolysis studies. Hart and Anbar (1960) give $E° = 2.77$ V for the reaction $e^-_{aq} + H^+ \rightarrow 1/2\, H_2$. Based on the reaction Cu II + OH → Cu III (Baxendale et al., 1965) and the calculations of Henglein (1974), a standard oxidizing potential, $E°$, of the order of 2 V may be associated with the OH radical. Reaction products with e^-_{aq} or OH frequently have only a transient existence, but recent developments permit recording time-resolved spectra on the nanosecond time scale (Schmidt et al., 1976).

The spectra of Sm^{2+}, Eu^{2+}, and Yb^{2+} in good agreement with fig. 24.16 have been obtained by several groups on the reduction of R^{3+}(aquo) with e^-_{aq} (Gordon, 1965; Faraggi and Tendler, 1972; and Pikaev, 1974). Pikaev et al. (1973) have also reported the reduction of Tm to the divalent state (pH 3–6) with a characteristic band at 280 nm ($\epsilon_{max} \sim 750\ M^{-1}\ sec^{-1}$). Both Faraggi and Feder (1972) and Pikaev et al. (1973) report the successful oxidation of Pr III to Pr IV on reaction with OH radicals. A characteristic intense absorption band was observed at 290 nm. Based on the trends in the potentials estimated by Nugent (1975), if the $OH + Pr^{3+} \rightarrow Pr^{4+}$ reaction can occur, then it should be possible to obtain Tb^{4+} under similar conditions.

Tendler and Faraggi (1972) used the pulse radiolysis technique to produce R^{2+}(aquo), and studied the rate of oxidation of R^{2+}(aquo) by NO_2^-. The results

were interpreted in terms of an outer sphere electron transfer mechanism and used to compute $E°$ for the R^{2+}/R^{3+} couple, but the values obtained are much too low. They also suggest an essentially constant (II–III) potential across the series except for those couples that have been measured. This was not confirmed by the results cited below, nor is it consistent with spectroscopic correlations (Nugent et al., 1973).

Recently Gordon et al. (1976) reexamined the reaction of e^-_{aq} with R^{3+}(aquo) in a study which included all of the lanthanides. Their rate constant data could be used to divide the series into three groups in terms of reactivity: (1) readily reduced ions Sm, Eu, Yb with rate constants in the range of 10^{10} M^{-1} sec^{-1}, (2) an intermediate group, Gd, Ho, Er, and Tm, with rate constants (10^7–10^8), and (3) a relatively unreactive group, Pr, Nd, Dy, Tb, and Lu with rate constants $\leq 10^6$. Using streak camera techniques they obtained the first spectroscopic evidence for Gd^{2+} and Ho^{2+}, fig. 24.18.

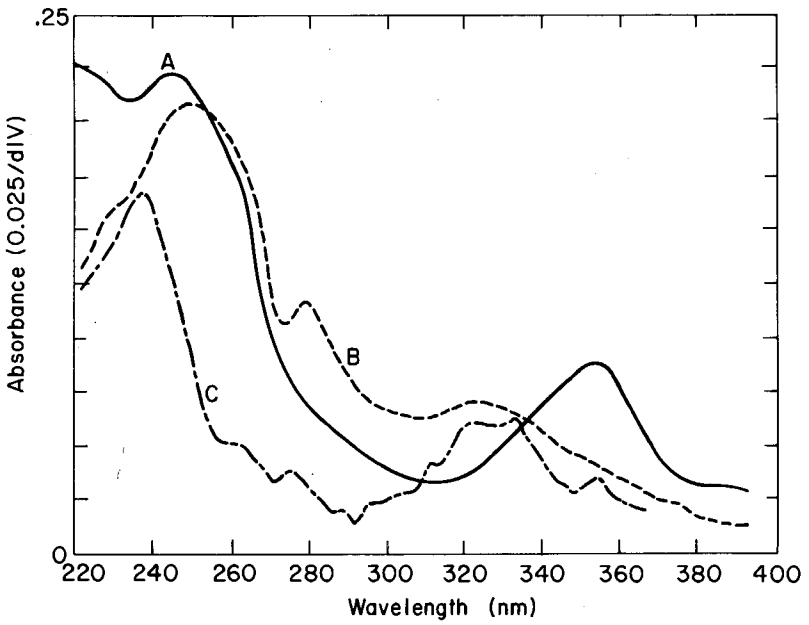

Fig. 24.18. Absorption spectra obtained by pulse radiolysis of lanthanide solutions. (A) Tm^{2+}, (B) Gd^{2+}, (C) Ho^{2+}, from Gordon et al. (1976).

References

Axe, J.D., 1963, J. Chem. Phys. **39**, 1154.
Banks, C.V. and D.W. Klingman, 1956, Anal. Chim. Acta **15**, 356.
Banks, C.V., M.R. Heusinkveld, J.W. O'Laughlin, 1961, Anal. Chem. **33**, 1235.
Barasch, G.E. and G.H. Dieke, 1965, J. Chem. Phys. **43**, 988.
Baxendale, J.H., E.M. Fielden, and J.P. Keene, 1965, Formation of CuIII in the Radiolysis of Cu^{2+} Solutions, in: A.J. Swallow and J.H. Baxendale, eds., Pulse Radiolysis, (Academic Press, London), p. 217.
Bertha, S.L. and G.R. Choppin, 1969, Inorg. Chem. **8**, 613.

Bethe, H.A. and F.H. Spedding, 1937, Phys. Rev. **52**, 454.
Bigeleisen, J., 1960, J. Chem. Phys. **32**, 1583.
Bodunov, E.N. and E.B. Sveshnikova, 1974, Opt. Spectrosc. **36**, 196.
Borkowski, R., H. Forest, and D. Grafstein, 1965, J. Chem. Phys. **42**, 2974.
Brewer, L., 1971a, J. Opt. Soc. Am. **61**, 1101.
Brewer, L., 1971b, J. Opt. Soc. Am. **61**, 1666.
Broer, L.J.F., C.J. Gorter, and J. Hoogschagen, 1945, Physica **11**, 231.
Butement, F.D.S., and H. Terrey, 1937, J. Chem. Soc., 1112.
Butement, F.D.S., 1948, Trans. Faraday Soc. **44**, 617.
Carnall, W.T., 1962, Anal. Chem. **34**, 786.
Carnall, W.T., D.M. Gruen, and R.L. McBeth, 1962, J. Phys. Chem. **66**, 2159.
Carnall, W.T., 1963, J. Phys. Chem. **67**, 1206.
Carnall, W.T., P.R. Fields and G.E. Toogood, 1964, J. Phys. Chem. **68**, 2351.
Carnall, W.T., P.R. Fields, and B.G. Wybourne, 1965, J. Chem. Phys. **42**, 3797.
Carnall, W.T., P.R. Fields, and K. Rajnak, 1968a, J. Chem. Phys. **49**, 4424, 4443, 4447, 4450.
Carnall, W.T., P.R. Fields and K. Rajnak, 1968b, J. Chem. Phys. **49**, 4412.
Carnall, W.T., 1974, Recent Developments in the Interpretation of Trivalent Lanthanide and Actinide Absorption Spectra, in: Trzebiatowska, B.J. and M. Rudolf, eds., Section Lectures of the Thirteenth International Conference on Coordination Chemistry, Polish Academy of Sciences, Warsaw, p. 89.
Carnall, W.T., H. Crosswhite, H.M. Crosswhite, and J.G. Conway, 1976, J. Chem. Phys. **64**, 3582.
Charlot, G., A. Collumeau, and M.J.C. Marchon, 1971, Selected Constants. Oxidation-Reduction Potentials of Inorganic Substances in Aqueous Solution, I.U.P.A.C., (Butterworths, London).
Choppin, G.R. and A.J. Graffeo, 1965, Inorg. Chem. **4**, 1254.
Christensen, R.J., J.H. Espenson, and A.B. Butcher, 1973, Inorg. Chem. **12**, 564.
Condon, E.U. and G.H. Shortley, 1957, The Theory of Atomic Spectra, (Cambridge Univ. Press, London) pp. 91–109.
Crosswhite, H.M., H. Crosswhite, and W.T. Carnall, 1975, Atomic Electronic Parameters Derived from Lanthanide and Actinide Crystal Spectra, in: Abstracts of the Atomic Spectroscopy Symposium, National Bureau of Standards, Gaithersburg, Md.
Crosswhite, H.M., H. Crosswhite, F.W. Kaseta, and R. Sarup, 1976, J. Chem. Phys. **64**, 1981.
Crosswhite, H.M. and R.D. Cowan, 1976, private communication.
Deutschbein, O. and R. Tomaschek, 1937, Ann. Physik. **29**, 311.
Dieke, G.H., 1968, Spectra and Energy Levels of Rare Earth Ions in Crystals, H.M. Crosswhite and H. Crosswhite, eds., (Wiley, New York).
Entelis, S.D. and R.P. Tiger, 1976, Reaction Kinetics in the Liquid Phase. (Wiley, New York), p. 71.
Ermolaev, V.L. and E.B. Sveshnikova, 1970, Opt. Spectry. **28**, 98.
Eyring, L., H.L. Lohr, and B.B. Cunningham, 1952, J. Am. Chem. Soc. **74**, 1186.
Faraggi, M. and Y. Tendler, 1972, J. Chem. Phys. **56**, 3287.
Faraggi, M. and A. Feder, 1972, J. Chem. Phys. **56**, 3294.
Fassel, V.A. and R.H. Heidel, 1954, Anal. Chem. **26**, 1134.
Franzen, P., J.P.M. Woudenberg, and C.J. Gorter, 1943, Physica **10**, 365.
Freed, S., 1931, Phys. Rev. **38**, 2122.
Freed, S. and S.I. Weissman, 1938, J. Chem. Phys. **6**, 297.
Freed, S., 1942, Rev. Mod. Phys. **14**, 105.
Freed, S. and C.J. Hochanadel, 1950, J. Chem. Phys. **18**, 780.
Freymann, R. and S. Takvorian, 1932, Compt. Rend. **194**, 963.
Gallagher, P.K., 1964, J. Chem. Phys. **41**, 3061.
Gallagher, P.K., 1965, J. Chem. Phys. **43**, 1742.
Geier, G., U. Karlen, and A. v. Zelewsky, 1969, Helv. Chem. Acta **52**, 1967.
Gobrecht, H. and R. Tomaschek, 1937, Ann. Physik. **29**, 324.
Gobrecht, H., 1938, Ann. d. Phys. **31**, 181.
Goldschmidt, R., G. Stein, and E. Würzberg, 1975, Chem. Phys. Ltrs. **34**, 408.
Gordon, S., 1965, in: A.J. Swallow and J.H. Baxendale, eds., Pulse Radiolysis, (Academic Press, London) p. 285.
Gordon, S., J.C. Sullivan, W.A. Mulac, D. Cohen, and K.H. Schmidt, 1976, Pulse Radiolysis of the Lanthanide and Actinide Elements, in: Proc. Fourth Symposium on Radiation Chemistry, Keszthely, Hungary.
Gruber, J.B. and J.G. Conway, 1960, J. Inorg. Nucl. Chem. **14**, 303.
Haas, Y. and G. Stein, 1971a, Chem. Phys. Ltrs. **11**, 143.
Haas, Y. and G. Stein, 1971b, J. Phys. Chem. **75**, 3677.
Haas, Y. and G. Stein, 1972, Chem. Phys. Ltrs. **15**, 12.
Haas, Y., G. Stein, and E. Würzberg, 1973, J. Chem. Phys. **58**, 2777.
Habenschuss, A. and F.H. Spedding, 1974, A Survey of Some Properties of Aqueous Rare Earth Salt Solutions. I. Volume, Thermal Expansion, Raman Spectra, and X-ray Diffraction, in: J.H. Haschke and H.A. Eick, eds., Proceedings of the 11th Rare Earth Research Conference, (Tech. Inform. Center, Oak Ridge, Tenn.) p. 909.
Halpern, J. and A.C. Harkness, 1959, J. Chem. Phys. **31**, 1147.
Hart, E.J. and M. Anbar, 1970, The Hydrated Electron, (Wiley-Interscience, N.Y.) p. 102 and 255.
Heller, A., 1966, J. Am. Chem. Soc. **88**, 2058.
Heller, A., 1968, J. Mol. Spectro. **28**, 208.
Hendrie, D.E., R.L. Fellows, and G.R. Choppin, 1976, Coord. Chem. Rev. **18**, 199.

Henglein, A., 1974, Ber. Bunsen-ges. für Physikal. Chemie, **78**, 1078.
Henry, B.R. and M. Kasha, 1968, Ann. Rev. Phys. Chem. **19**, 161.
Hinchley, R.J. and J.W. Cobble, 1970, Inorg. Chem. **9**, 917.
Hindman, J.C. and J.C. Sullivan, 1971, Principles and Methods for the Study of Metal Complex Ion Equilibrium, in: Martell, A.E. ed., Coordination Chemistry, Vol. 1, ACS Monograph 168, (Van Nostrand Reinhold, N.Y.), Chapter 7.
Holleck, L. and C. Hartinger, 1955, Angew. Chemie, **67**, 648.
Hoogschagen, J., A.P. Snoek, and C.J. Gorter, 1943, Physica **10**, 693.
Hoogschagen, J., 1946, Physica **11**, 513.
Hoogschagen, J., A.P. Snoek, and C.J. Gorter, 1946, Physica **11**, 518.
Hoogschagen, J., Th. G. Scholte, and S. Kruyer, 1946, Physica **11**, 504.
Hoogschagen, J. and C.J. Gorter, 1948, Physica **14**, 197.
Hornig, D.F., H.F. White, and F.P. Redding, 1958, Spectrochim. Acta **12**, 338.
Johnson, K.E. and J.N. Sandoe, 1968, Can. J. Chem. **46**, 3457.
Jørgensen, C.K., 1955, Dan. Mat. Fys. Medd. **29**, No. 11.
Jørgensen, C.K. and J.S. Brinen, 1963, Mol. Phys. **6**, 629.
Jørgensen, C.K., 1969, Oxidation Numbers and Oxidation States, (Springer-Verlag, Berlin).
Jørgensen, C.K., 1973, Struct. Bonding **13**, 199.
Jørgensen, C.K. and B.R. Judd, 1964, Mol. Phys. **8**, 281.
Jørgensen, C.K., 1976, Private communication.
Judd, B.R., 1962, Phys. Rev. **127**, 750.
Judd, B.R., 1963, Operator Techniques in Atomic Spectroscopy, (McGraw-Hill, N.Y.).
Judd, B.R., 1966a, Phys. Rev. **141**, 4.
Judd, B.R., 1966b, J. Chem. Phys. **44**, 839.
Judd, B.R., H.M. Crosswhite, and H. Crosswhite, 1968, Phys. Rev. **169**, 130.
Karraker, D.G., 1970, J. Chem. Ed. **47**, 424.
Kazanskaya, N.A. and E.B. Sveshnikova, 1970, Opt. Spectry. **28**, 376.
Kondrat'eva, E.V., 1960, Opt. Spectry. **8**, 66.
Kondrat'eva, E.V. and G.S. Lazeeva, 1960, Opt. Spectry. **8**, 67.
Kropp, J.L. and M.W. Windsor, 1963, J. Chem. Phys. **39**, 2769.
Kropp, J.L. and M.W. Windsor, 1965, J. Chem. Phys. **42**, 1599.
Kropp, J.L. and W.R. Dawson, 1966, J. Chem. Phys. **45**, 2419.
Kropp, J.L. and M.W. Windsor, 1966, J. Chem. Phys. **45**, 761.
Kropp, J.L. and M.W. Windsor, 1967, J. Phys. Chem. **71**, 477.
Laitinen, H.A. and W.A. Taebel, 1941, Ind. Eng. Chem., Anal. Ed. **13**, 825.
Laitinen, H.A., 1942, J. Am. Chem. Soc. **64**, 1133.
Lang, R.J., 1936, Can. J. Research **14A**, 127.
Lange, H., 1938, Ann. d. Phys. **31**, 609.
Lewis, W.B., J.B. Mann, D.A. Liberman, D.T. Cromer, 1970, J. Chem. Phys. **53**, 809.
Main-Smith, J.D., 1927, Nature **120**, 583.
Mamiya, M., 1965, Bull. Chem. Soc. Japan **38**, 178.
Martin, W.C., 1971, J. Opt. Soc. Am. **61**, 1682.
Moeller, T. and J.C. Brantley, 1950, Anal. Chem. **22**, 433.
Morrison, J.C. and K. Rajnak, 1971, Phys. Rev. **A4**, 536.
Morss, L.R. and H.O. Haug, 1973, J. Chem. Thermodyn. **5**, 513.
Mukherji, P.C., 1936, Indian J. Phys. **10**, 319.
Newman, D.J. and C.D. Taylor, 1971, J. Phys. B **4**, 241.
Newman, D.J. and C.D. Taylor, 1972, J. Phys. B **5**, 2332.
Nielson, C.W. and G.F. Koster, 1963, Spectroscopic Coefficients for p^n, d^n, and f^n Configurations, (M.I.T. Press, Cambridge).
Nugent, L.J. and K.L. VanderSluis, 1971, J. Opt. Soc. Am. **61**, 1112.
Nugent, L.J., R.D. Baybarz, J.L. Burnett, J.L. Ryan, 1973, J. Phys. Chem. **77**, 1528.
Nugent, L.J., 1975, Chemical Oxidation States of the Lanthanides and Actinides, in: Bagnall, K.W., ed., International Review of Science, Inorganic Chemistry Series Two, Vol. 7, (University Park Press, Baltimore), Chapter 6.
Ofelt, G.S., 1962, J. Chem. Phys. **37**, 511.
Peacock, R.D., 1975, Struct. Bonding **22**, 83.
Pikaev, A.K., G.K. Sibirskaya, V.I. Spitsyn, 1973, Dokl. Akad. Nauk SSSR, **209**, 1154.
Pikaev, A.K., 1974, Rad. Res. Reviews **5**, 177.
Prandtl, W. and K. Scheiner, 1934, Zeit. Anorg. Allgem. Chem. **220**, 107.
Rajnak, K. and B.G. Wybourne, 1963, Phys. Rev. **132**, 280.
Rard, J.A. and F.H. Spedding, 1974, A Survey of Some Properties of Aqueous Rare Earth Salt Solutions. II. Heats of Dilution, Heat Capacities, Activity Coefficients, Electrical Conductances, and Relative Viscosities, in: J.H. Haschke and H.A. Eick, eds., Proceedings of the 11th Rare Earth Research Conference, (Tech. Inform. Center, Oak Ridge, Tenn.) p. 919.
Reuben, J. and D. Fiat, 1969a, J. Chem. Phys. **51**, 4909.
Reuben, J. and D. Fiat, 1969b, J. Chem. Phys. **51**, 4918.
Riseberg, L.A. and H.W. Moos, 1968, Phys. Rev. **174**, 429.
Robinson, G.W. and R.P. Frosch, 1963, J. Chem. Phys. **38**, 1187.
Rosseinsky, D.R., 1965, Chem. Rev. **65**, 467.
Ryan, J.L. and C.K. Jørgensen, 1966, J. Phys. Chem. **70**, 2845.
Satten, R.A., 1953, J. Chem. Phys. **21**, 637.
Sayre, E.V., D.G. Miller, and S. Freed, 1957, J. Chem. Phys. **26**, 109.
Schmidt, K.H., S. Gordon, and W.A. Mulac, 1976, Rev. Sci. Instrum. **47**, 356.
Selwood, P.W., 1930, J. Am. Chem. Soc. **52**, 4308.
Siebrand, W., 1967, J. Chem. Phys. **46**, 440.

Sonesson, A., 1958, Acta Chem. Scand. **12**, 165, 1937.
Spedding, F.H., 1940, Phys. Rev. **58**, 255.
Spedding, F.H., P.F. Cullen, and A. Habenschuss, 1974, J. Phys. Chem. **78**, 1106.
Stein, G. and E. Würzberg, 1975, J. Chem. Phys. **62**, 208.
Stewart, D.C., 1959, Absorption Spectra of Lanthanide Rare Earths, in: Pascal, P. ed., Nouveau Traité de Chemie Minerale, Vol. 7, Part II, (Masson et C^{ie}, Paris), p. 1201.
Sveshnikova, E.B. and V.L. Ermolaev, 1971, Opt. Spectry. **30**, 208.
Tendler, Y. and M. Faraggi, 1972, J. Chem. Phys. **57**, 1358.
Tomaschek, R., 1932, Physik. Zeitschr. **33**, 878.
Tomaschek, R. and O. Deutschbein, 1933, Physik. Zeitschr. **34**, 374.
Tomaschek, R. and E. Mehnert, 1937, Ann. Phys. **29**, 306.
Tomaschek, R., 1939, Faraday Soc. Trans. **35**, 148.
Tomaschek, R., 1942, Ergeb. exakt. Naturwiss. **20**, 268.
Trees, R.E., 1964, J. Opt. Soc. Am. **54**, 651.
Van Vleck, J.H., 1937, J. Phys. Chem. **41**, 67.
Woudenberg, J.P.M., 1942a, Physica **9**, 217.
Woudenberg, J.P.M., 1942b, Physica **9**, 936.
Wybourne, B.G., 1965, Spectroscopic Properties of Rare Earths, (Wiley, N.Y.).
Young, J.P. and J.C. White, 1960a, Anal. Chem. **32**, 799.
Young, J.P. and J.C. White, 1960b, Anal. Chem. **32**, 1658.
Zaidel, A.N., 1937, Nature, **139**, 248.
Zaidel, A.N., Ya. I. Larionov, and A.N. Filippov, 1938, J. Gen. Chem. (USSR) **8**, 943.
Zaidel, A.N. and Ya. I. Larionov, 1939, Uspekki Fiz. Nauk **21**, 211.
Zaidel, A.N. and Ya.I. Larionov, 1943, Trudy Vsesoyuz. Konferentsii Anal. Khim. **2**, 615.